MAST

OAK RIDGE NATIONAL LABORATORY

operated by

UNION CARBIDE CORPORATION

for the

U.S. ATOMIC ENERGY COMMISSION

ORNL- TM- 292

/3-3

UNIT OPERATIONS SECTION MONTHLY PROGRESS REPORT

APRIL 1962

ORNL-TM-292

UNIT OPERATIONS SECTION MONTHLY PROGRESS REPORT

April 1962

CHEMICAL TECHNOLOGY DIVISION

M. E. Whatley

P. A. Haas
R. W. Horton
A. D. Ryon
J. C. Suddath
C. D. Watson

Date Issued

OCT - 8 1962

ABSTRACT

Bubble size measurements in the foam column showed that a spinnerette with 50 μ holes gave a nearly normal distribution of bubbles sizes while a coarse fritted glass gas sparger had a tail of large bubbles which did not fit the normal curve. A set of equations solvable by a finite difference technique are presented which completely describe the irreversible reaction rate of H_2 or CO with a fixed bed of CuO pellets. Radiation damage tests are in progress to evaluate plastics for the Transuranium program. All dejacketed SRE Core I uranium fuel slugs have been recanned and shipped to Savannah River. Installation of the shear-leach complex is complete. The shortest practical length into which a tubular fuel element assembly may be sheared appears to be 1/2 in. Tests showed difficulties with shearing assemblies containing tube sheets. The stepped shear blade used for Mark I prototype fuel elements produced chunks of porcelain filled Yankee prototypes. Flow capacities of nozzle plate pulsed columns operated under dilute Purex flowsheet conditions were determined. Fuel pins made with compacted sol-gel thorium dioxide and U-235 have been irradiated without difficulty to 17,000 megawatt days/ton. Routine operation of the rotary denitrator to give thorium dioxide product was demonstrated.

CONTENTS

Previous Reports in this Series for the Years 1961-1962

January	ORNL CF 61-1-27
February	ORNL CF 61-2-65
March	ORNL CF 61-3-67
April	ORNL-TM-32
May	ORNL-TM-33
June	ORNL-TM-34
July	ORNL-TM-35
August	ORNL-TM-65
September	ORNL-TM-112
October	ORNL-TM-121
November	ORNL-TM-122
December	ORNL-TM-136
January	ORNL-TM-150
February	ORNL-TM-157
March	ORNL-TM-222

All previous reports in this series are listed in the
June 1961 report, ORNL-TM-34, from the beginning,
December 1954.

SUMMARY

1.0 CHEMICAL ENGINEERING RESEARCH

Foam Separation

Bubble size distributions were measured from photographs 2-5 cm above the foam-liquid interface where the bubbles were still spherical instead of polyhedrons. While distributions from the spinnerette with 50 μ holes were close to normal distributions ($\mu = 0.53$ mm, $\sigma = 0.08$); those from extra coarse fritted glass gas spargers had a tail of large bubbles which did not fit a normal curve. A 0.4 in. dia cyclone tested as a foam breaker had a feed capacity of 14 liters/min for an inlet/ outlet pressure ratio of about 4. The uncondensed foam volume was from $< 0.2\%$ for dry foam up to 4% of the feed foam volume for wet foam. Foam densities from 3 to 30 mg/cc after drainage in a 1 ft length of column were observed with the linear foam velocity and the immediate past history of the solution as the most important variables. The foam density at the start of a run was as much as six times the steady state density for the same conditions with recycle of the condensed foam.

2.0 GCR COOLANT PURIFICATION STUDIES

Variables effecting the fast, irreversible reaction of H_2 or CO with a fixed bed of CuO pellets were grouped in dimensionless parameters and substituted in the kinetic equation that completely describes the system, resulting in three equations that are solvable by a finite difference technique.

Correlation of co-sorption data is being attempted using a kinetic model of mass transport of the H_2O and CO_2 from the bulk gas stream being the controlling mechanism for sorption.

3.0 POWER REACTOR FUEL PROCESSING

3.1 Transuranics - Material Evaluation

Radiation damage tests are in progress to evaluate protective coatings, plastic materials of construction and flooring for possible use in the proposed Transuranic facility. A satisfactory flooring system has not yet been found.

3.2 Mechanical Dejacketing of SRE Core I Fuel

All dejacketed SRE Core I uranium fuel slugs which were experimentally dejacketed and recanned in aluminum have been transferred to the Savannah River Plant for chemical reprocessing. Developmental work with this fuel is completed.

3.3 Shear and Leach

Installation of the shear-leach complex and chemical processing equipment is completed including check out of the electrical circuitry for both manual and automatic operation.

There was no appreciable difference in particle distribution between porcelain filled ORNL Mark I fuel elements assembled with Nicrobraz-50 and those assembled with Kanigen braze. A comparison of the particle distribution from the sheared lengths of 1, 3/4, 1/2 and 1/4 in. showed 11, 16, 33, and 69%, respectively, of particles < 9520 microns and 1.5, 2.4, 4.3, and 5.2%, respectively, for < 44 microns. The shortest practical length into which a tubular fuel assembly may be sheared appears to be 1/2 in. The void fraction of randomly packed sheared pieces obtained by shearing a total length of 8 in. from a porcelain filled ORNL Mark I fuel assembly into 1/4, 1/2, 5/8, 3/4, 1, and 1-1/2 in. lengths is 0.42 for the 1/4 in. pieces and about 0.575 for the remaining lengths.

Trial 1 in. long shearings of three ORNL Mark I porcelain filled proto-types containing 1/8 in. stainless steel tube sheets located 1/2 in. from each end, show that the tube sheets prevent the separation of the sheared tubes. A large section containing 25 tubes damaged the adjustable stop of the shear on the return stroke. Tests with the 6 tube sheets indicate that it may not be advisable to attempt to shear fuel assemblies containing tube sheets.

The stepped blade of the shear which normally creates discrete pieces of sheared tubing from a Mark I produced some tubular chunks during the successful shearing of three porcelain filled Yankee prototypes. The center step of the blade appears to be too wide for this fuel type. The blade performs well after having made 4507 cuts on a 36 tube Mark I proto-type.

Power measurements indicate that a maximum power of 26.5 hp is required to shear through a row of ferrules of a porcelain filled Mark I prototype fuel assembly with Nicrobraz-50 as the bonding agent.

4.0 SOLVENT EXTRACTION STUDIES

Flow capacities of nozzle plate pulse columns operated under dilute purex flowsheet conditions were determined. The flow capacity for a 23% free area nozzle plate column when operated as a compound extraction scrub column, increased from < 420 to 875 gal $ft^{-2}hr^{-1}$ as the pulse frequency decreased from 70 to 35 cpm, and when operated as a simple extraction column increased from 680 to 875 gal $ft^{-2}hr^{-1}$ as pulse decreased from 50 to 35 cpm. The flow capacity for a 10% free area nozzle plate operated as a simple extraction column increased from 350 to 560 gal $ft^{-2}hr^{-1}$ as the pulse frequency decreased from 50 to 35 cpm. The solvent flow capacity of nozzle plate columns operated under dilute purex flowsheet conditions was 30 to 40% of that obtained in the same columns with the standard purex flowsheet. Flow capacity of the stripping column (10% free area nozzle plate, aqueous continuous operation) with the nozzles oriented downward was slightly higher at low pulse frequencies than when the nozzles were oriented up (1370 vs 1170 gal $ft^{-2}hr^{-1}$ and 25 cpm) but were approximately the same at higher pulse frequencies (550 vs 600 gal $ft^{-2}hr^{-1}$ at 50 cpm).

5.0 THORIUM UTILIZATION STUDIES

Fuel pins containing sol-gel $ThO_2(U-235)O_2$ vibratorily compacted to 8.6-8.7 g/cc have been irradiated without difficulty to 10,000-17,000 megawatt days/ton of Th in the NRX and MTR reactors. These 11 in. long, 5/16 in. o.d. specimens have been at cladding heat fluxes of 200,000-600,000 $Btu/hr \cdot ft^2$. Two capsules containing sol-gel $ThO_2-U(235)O_2$ in the ORR pool side facility are at cladding temperatures of 1000°F and 1300°F and centerline temperatures of 2700-3600°F. Routine operation of the rotary denitrator to give ThO_2 product excellent for dispersion into sols was demonstrated. A rapid initial heating to 180°C in the absence of steam appeared to eliminate the previously obtained undesirable creamy fraction. Satisfactory operation of the Kilorod scale calcination-reduction furnace was demonstrated. Preparation of thoria-urania sol by dispersion of denitrator product in $UO_2(NO_3)_2$ solution was tested.

1.0 CHEMICAL ENGINEERING RESEARCH

1.1 Foam Separation - P. A. Haas, D. A. McWhirter

Engineering studies of the problems associated with design and operation of foam columns were continued in 6-in.-i.d. columns. Experimental runs were made to determine the height of a transfer unit as a function of flow rates, bubble sizes, and liquid feed distribution. The bubble size distributions, the performance of a cyclone foam breaker, and the drainage of foam were studied individually.

Bubble Size Distributions. The more uniform bubble diameters from use of the spinnerette as compared to extra-coarse sintered glass gas spargers was shown by photographs printed with a mm grid (Figures 1.1 and 1.2). These photographs were taken 2-5 cm above the liquid-foam interface with 500 cc/min of countercurrent liquid flow and 800 cc/min of N_2 through the spinnerette with 1850 50 μ dia holes or through two extra coarse fritted glass cylinder gas dispersors. The gas bubbles were separated by liquid and were approximately spherical when this close to the interface or when high countercurrent liquid rates were used. The effects of foam breakage were minimized and the diameters were easier to measure for these spherical bubbles as compared to the polyhedrons which resulted as liquid drains from the foam.

The bubble size distribution from the spinnerette is reasonably well represented by normal distributions, but the EC fritted glass gas spargers give a tail of large bubbles which normal distributions will not represent (Figure 1.3). Previously used "D" porosity sintered stainless steel (65 μ mean pore openings) give mean bubble diameters near those of the spinnerette, but the distribution is much broader with many bubbles over 1 mm dia.'

The uniform bubbles from the spinnerette give a much more stable foam than the irregular bubbles from the fritted glass or sintered stainless steel. A foam is not by nature a stable geometry and large bubbles appear to grow at the expense of small ones thus reducing the foam surface. The cost of the spinnerettes is not excessive (about 5 ¢/hole for fabrication and 5 ¢/hole for the Au-Pt alloy or $160-180 for the 6 in. dia column) and their use appears more necessary as the column size is increased.

Cyclone Foam Breaker. Experimental data were collected for foam breaking by the 0.40 in. i.d. cyclone as initially used for the 6 in. dia foam column. Foam generated at 500-1400 cc/min using "D" porosity sintered stainless steel gas spargers and 300 to 1500 ppm Trepolate F-95 was drawn through the cyclone by vacuum with the top of the column vented to the atmosphere (Figure 1.4). The capacity for feed foam at atmospheric pressure and ~22 in. Hg vacuum in the collection pot was 14,000 cc/min foam; the capacity for foam free air would be about 30 liter/min for these pressures.
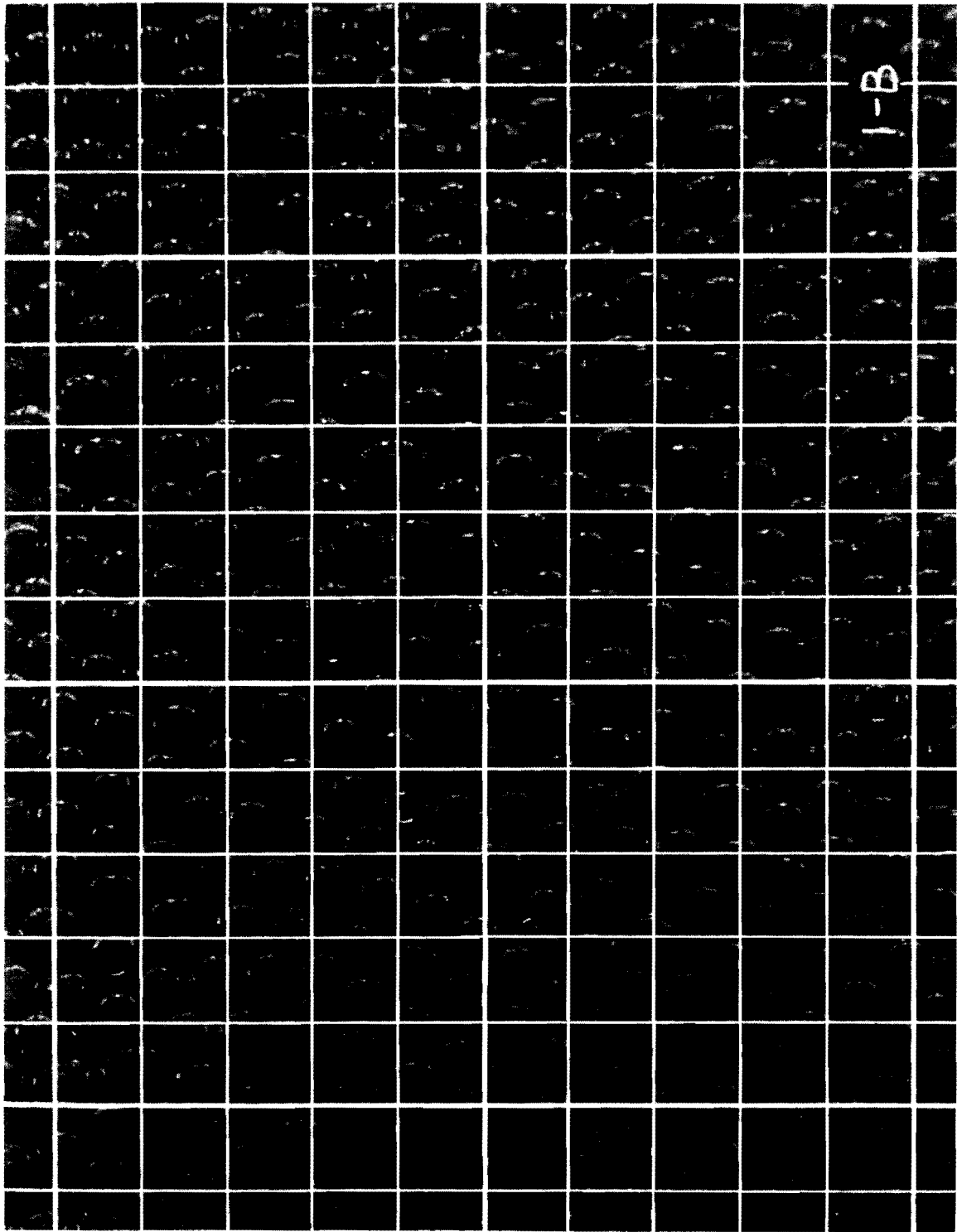
Fig. 1.1. Foam from N_2 through 50μ dia holes of spinnerette into 275 ppm trepolate F-95 in 10^{-3} M NaOH; 1 mm grid or approximately 16 x magnification.
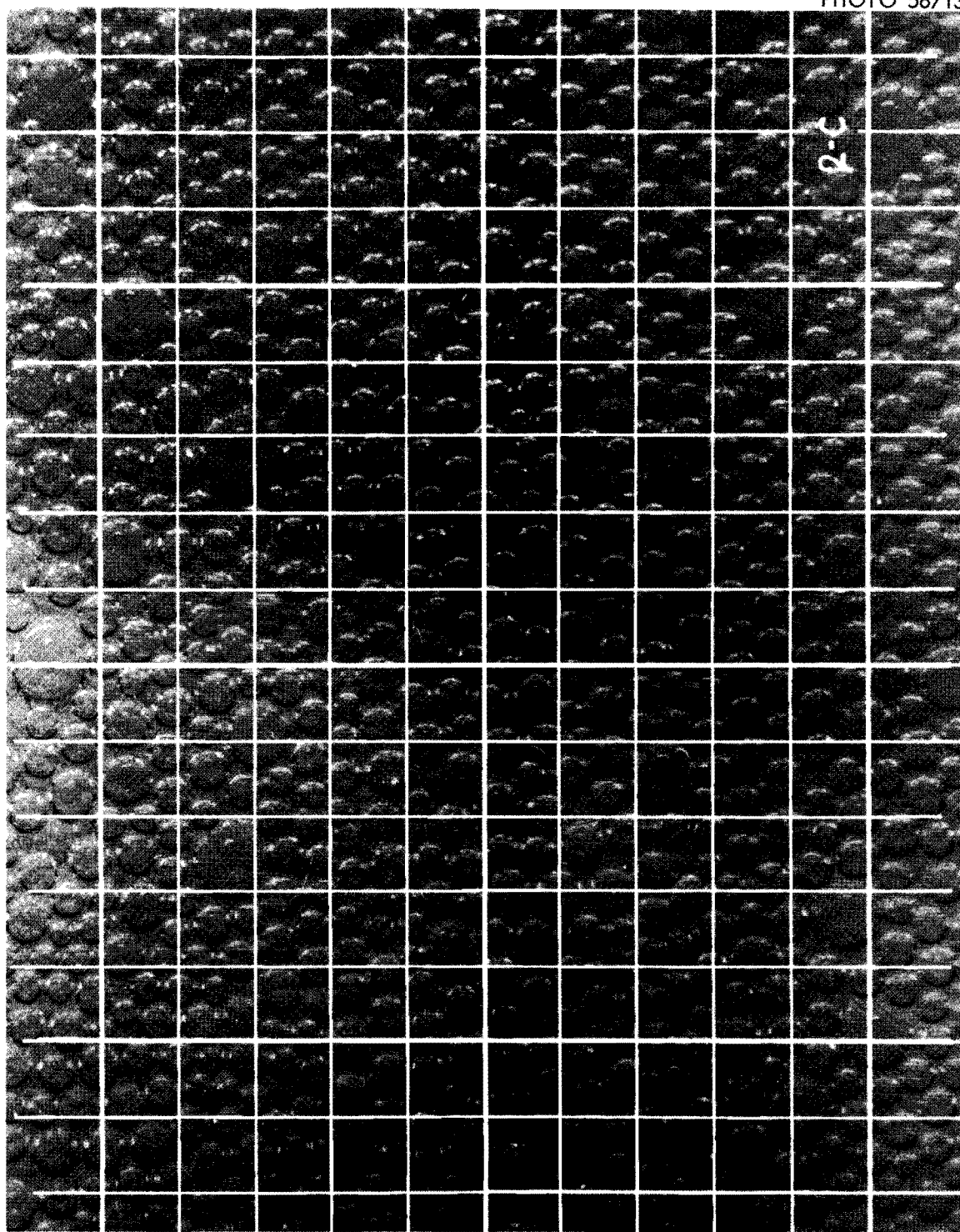
Fig. 1.2. Foam from N_2 through extra-coarse sintered glass gas spargers into 275 ppm trepolate F-95 in 10^{-3} M NaOH; 1 mm grid or approximately 16 x magnification.
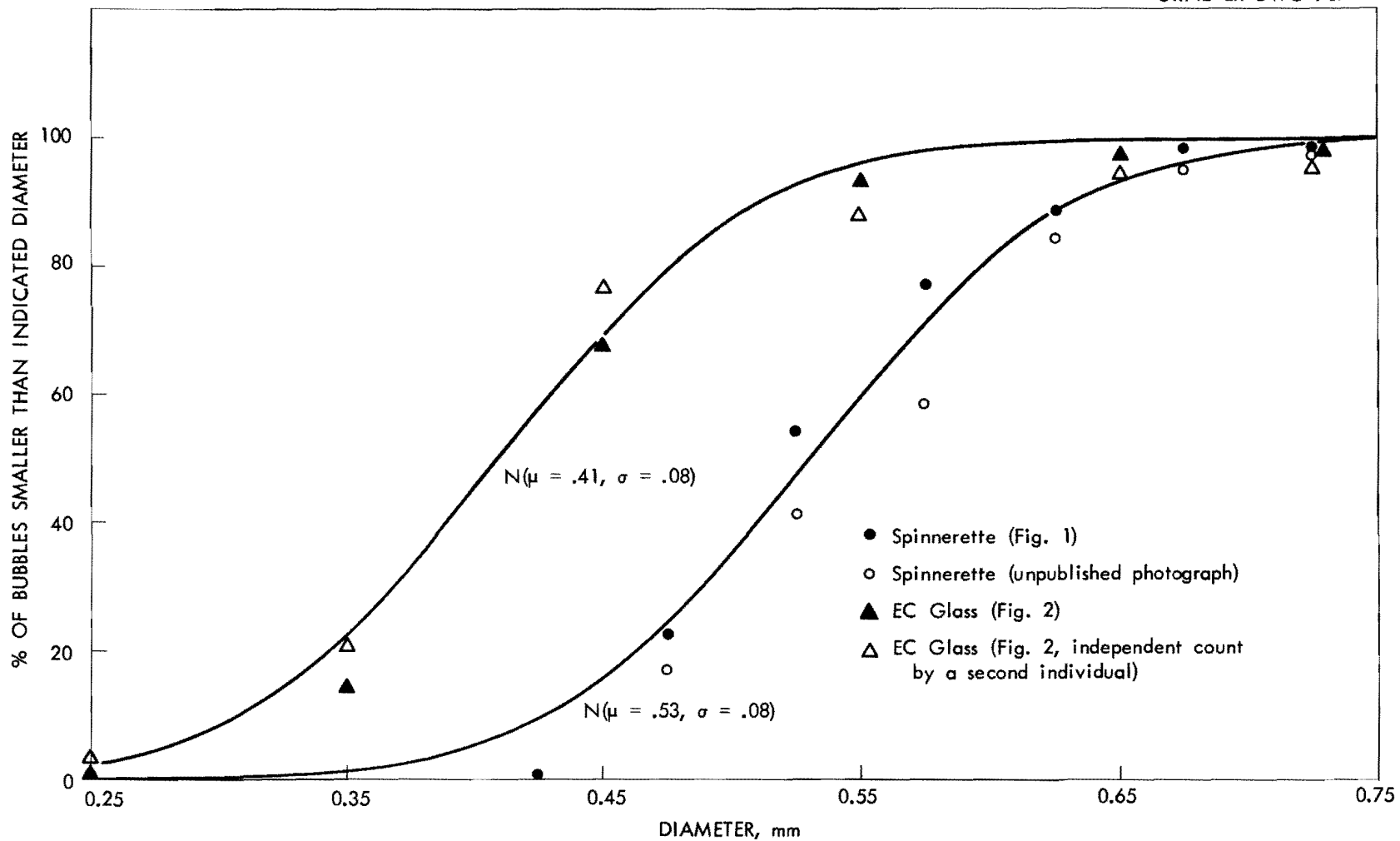
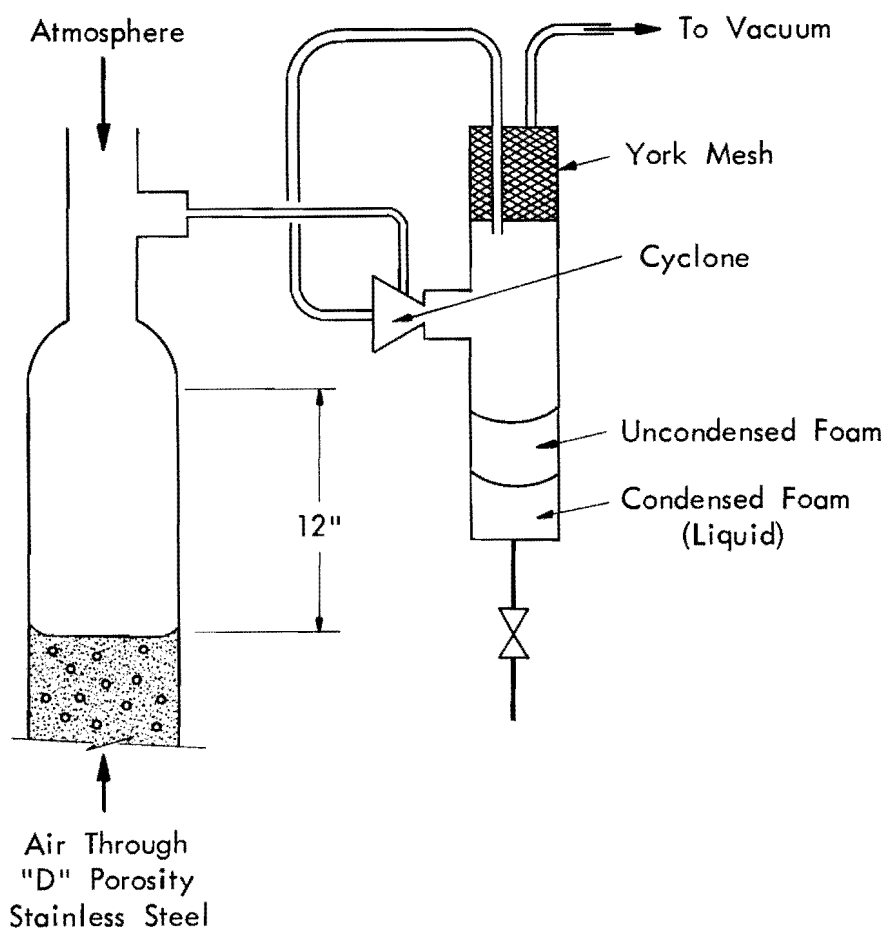Fig. 1.3. Bubble distributions for N_2 in 275 ppm trepolate F-95, 0.001 M NaOH.

Fig. 1.4. Cyclone foam breaker apparatus.

The effectiveness of foam breaking appeared to decrease as the wetness of the foam increased. The uncondensed foam was a wet, slow-to-break foam of very small bubble diameter. For collection periods of 10 min, the volumes of uncondensed foam (measured at atmospheric pressure) compared to the feed foam volumes were < 0.2% for 500-800 cc/min foam rates and usually 0.4-1.0% for 1200-2000 cc/min foam rate, and for 20 liters of feed foam, 1-4% for 4000-8000 cc/min foam rate. The data did not reproduce well and variations by factors of two for identical conditions were common. The variations with surfactant concentrations were not significant. Addition of 20 cc/min of H_2O to the cyclone feed line for foam rates of 1000, 2000, and 4000 cc/min resulted in a small increase in the volume of uncondensed foam.

A pump was used to pump the liquid and foam as they collected from the cyclone receiver pot to a settler with overflow of the foam to the cyclone feed line. The results indicate that such an arrangement would permit application of cyclone foam breakers without removal of uncondensed foam from the system. The gas to generate the foam and to operate the cyclone could be recycled to contain contamination or to minimize inert gas requirements if an inert atmosphere was desired.

Foam Drainage. Foam density data has not been published for dodecylbenzenesulfonate surfactant although some data is available for other systems.* Therefore, the cyclone foam breaker tests reported in the previous section were planned to also give foam density data. The rate of condensed foam collection corrected for a small amount of evaporation in the cyclone was divided by the gas rate to give the foam density. The 8 liters of liquid in the 6 in. dia pot in which the foam was generated would not change significantly in surfactant concentration during a rate determination and the condensed foam was returned prior to the following determination. There was about 1 ft of 6 in. dia. column for foam drainage between the interface and the takeoff to the cyclone (Figure 1.4).

Variations in the foam densities with the linear foam rate during drainage, the pH, and the surfactant concentrations were expected, but the immediate previous history of the solution was an unexpectedly important variable. While reproducible foam densities were obtained after foaming and return of the condensed foam bed continued for long periods, the initial foam densities with new solution or for solution which had stood overnight were as much as six times greater than the reproducible steady state values (Figure 1.5). The results in Table 1.1 and the points for < 0.4 hr in Figure 1.5 illustrate the type of behavior observed. One explanation possible is that interaction of the surfactant with the water at a relatively slow rate results in a structure which hinders drainage of water from the foam.

The steady state foam densities appeared directly proportional to the superficial gas velocities over the range studied (Figure 1.5).

*ORNL-TM-1, Chemical Technology Division, Chemical Development Section B Quarterly Progress Report, April-June, 1961, p. 68-69.
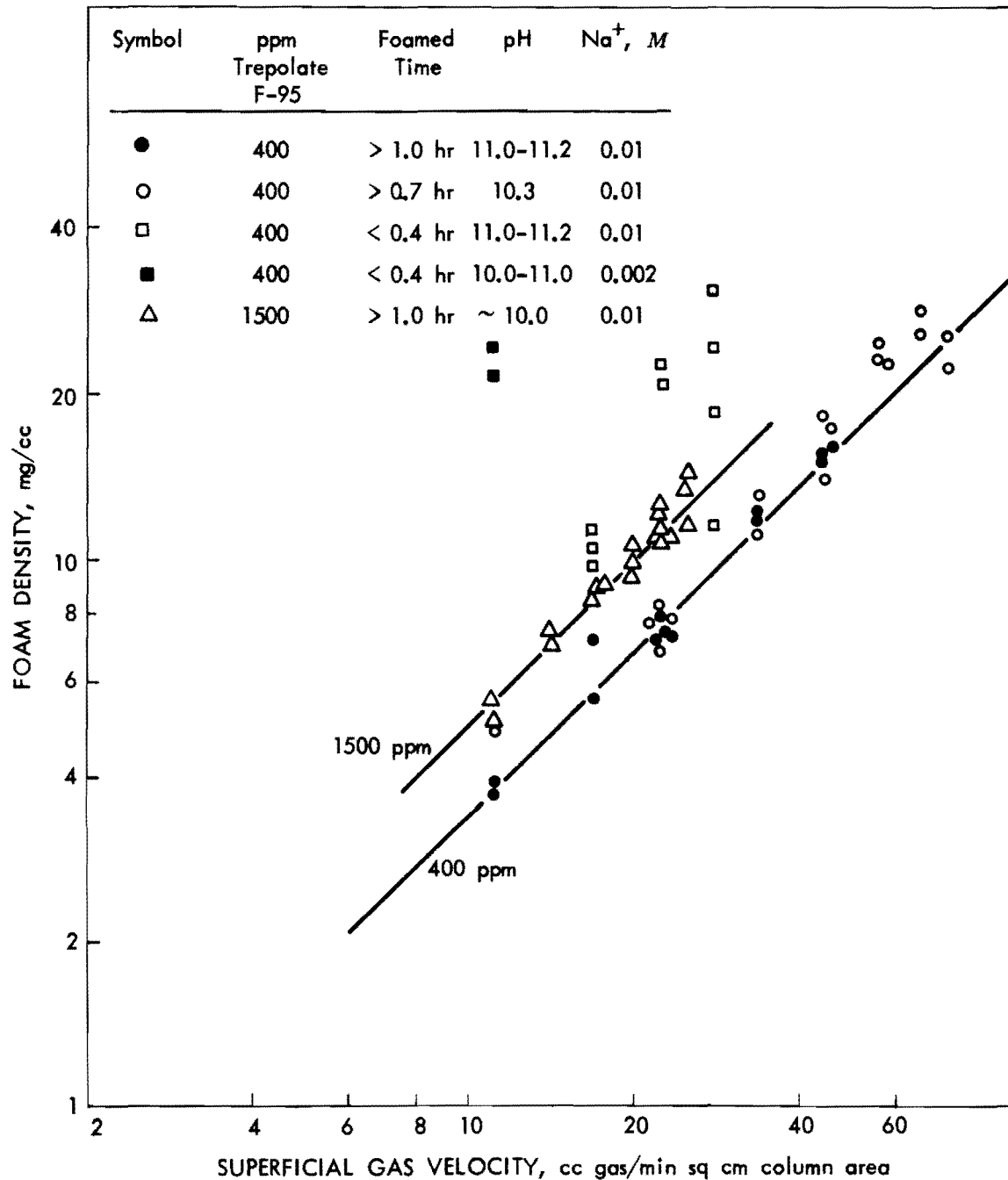
Fig. 1.5. Foam densities for a dodecylbenzenesulfonate surfactant, foam of about 0.6 mm dia. Conditions: batch charge of solution; "D" porosity stainless steel gas sparger; one foot of column for foam drainage.

Table 1.1. Foam Densities for a Dodecylbenzenesulfonate Surfactant

Conditions: Trepolate F-95 Surfactant, about 0.01 $\underline{N}$ Na^+
and pH of 10-11. The 400 ppm solution was
not foamed previously; the 1500 ppm solution
was used the previous day and stood overnight.
Gas rate of 4000 cc/min or 221 cm/sec super-
ficial velocity.

Accumulated Time, min	Foam Density, mg/cc, or Remarks, 400 ppm Trepolate F-95	Foam Density, mg/cc, or Remarks, 1500 ppm Trepolate F-95
0	Foam gas started	Foam gas started
6-15	23	22,21
65	8.6	-
165-180	-	10.9, 10.9, 12.1
190-200	7.7	11.4, 10.6, 12.4
205	-	Foam gas shut off
245	-	Foam gas started
249-254	-	21.2, 19.8, 23.0
267-270	-	19.8, 16.8, 15.3
290-305	7.3	12.5, 12.5, 12.0
400	7.3	-
410	Foam gas shut off	-
1515	Foam gas started	-
1523	21.7	-
1580	8.2	-
1665	6.8	-
1685	Foam gas shut off	-
1700	Foam gas started	-
1708	9.3	-

Measurements at lower foam rates were not practical because of the excessive foam breakage of the irregular bubbles from the porous stainless steel gas spargers. The foam densities of 1500 ppm of Trepolate were 150% of the densities for 400 ppm Trepolate. No consistent effects on foam densities were observed for the variation of NaOH and NaHCO$_3$ concentrations from 0 to 0.01 $\underline{M}$ to give pH values of 10-11.5 and Na concentrations of 0.002-0.01.

The purpose of observing foam densities was to obtain an indication of what foam linear velocities would be required for the drainage sections of countercurrent columns. The great sensitivity of the foam density to the immediate previous history of the solution means that obtaining valid foam density values will probably require a close simulation of the column geometry and holdup times using a continuous liquid feed. Such a study would not be justified until the conditions and solutions to be used in a large column were well known. The condensed foam rates from the countercurrent column runs (275 ppm Trepolate F-95, 18-24 in. of 6 in. dia drainage section) can be used to calculate foam densities for 10-17 cm/sec superficial gas velocities. The values calculated approximate the values given by the 1500 ppm line of Figure 1.5 and thus appear to be 2-3 times the values which would be expected from extrapolation of the steady state values of Figure 1.5 to 275 ppm and 18-24 in. drainage length.

2.0 GCR COOLANT PURIFICATION STUDIES

J. C. Suddath

2.1 Reaction of H_2 or CO with Fixed Beds of CuO Pellets - C. D. Scott

It is desirable to develop generalized mathematical expressions for the kinetic model of external film diffusion and internal pore diffusion controlling the rapid, irreversible reaction of a fluid species from a flowing stream of fluid with fixed beds of porous solid particles. Specifically it is desirable to have these expressions for use in the systems of H_2 or CO in a flowing stream of helium reacting with fixed beds of CuO pellets. The results of such generalized expressions have much more general utilization in other reaction systems and they result in a simpler method of correlation of the effects of parameters.

The three differential equations which describe the system were previously derived:[1] Material Balance Equation

$$\left(\frac{\partial c}{\partial t}\right)_z + u \left(\frac{\partial c}{\partial z}\right)_t = -\frac{1}{\epsilon} \left(\frac{\partial n}{\partial t}\right)_z \tag{1}$$

Specific Reaction Rate Equation

$$\left(\frac{\partial n}{\partial t}\right)_z = kaC \left[1 - \frac{ka\,(r_e - r_i)}{4\pi a D \tau\, r_e r_i + ka\,(r_e - r_i)}\right] \tag{2}$$

Reaction Interface Equation

$$\left(\frac{\partial r_i}{\partial t}\right)_z = -\frac{1}{4\pi b \tau r_i^2} \left(\frac{\partial n}{\partial t}\right)_z \tag{3}$$

where,

> a = effective mass transfer area between fluid and CuO pellets, cm^2/cm^3
>
> b = molar density of CuO in pellet phase, $g\text{-moles}/cm^3$
>
> C = concentration of fluid species of interest in the fluid phase, $g\text{-moles}/cm^3$
>
> D = molecular diffusivity of fluid species of interest, cm^2/sec
>
> k = mass transfer coefficient across external gas film, cm/sec
>
> n = content of reacted phase in the pellet phase, $g\text{-moles}/cm^3$

r_e = radius of equivalent pellet sphere, cm

r_1 = radial distance of reaction interface within equivalent pellet sphere, cm

t = time, sec

u = interstitial fluid velocity, cm/sec

z = distance in column above fluid entrance, cm

α = effective internal pellet porosity

ϵ = external bed porosity

τ = specific average pellet density in bed, pellets/cm^3

The material balance equation, eq. (1), can be reduced in complexity in a manner similar to that of Vermeulen[2] by considering the following changes in variables:

$$v = Az \tag{4}$$

$$Q = Ft \tag{5}$$

where,

A = cross sectional area of the column, cm^2

F = volumetric flow rate of gas, cm^3/sec

v = volume of bed up to a distance z above the bottom of the bed, cm^3

Q = volume of gas fed to column up to time t, cm^3

Then eq. (1) becomes

$$\epsilon \left(\frac{\partial C}{\partial Q}\right)_v + \left(\frac{\partial C}{\partial v}\right)_Q = - \left(\frac{\partial n}{\partial Q}\right)_v \tag{6}$$

Now consider the new variable, $(Q - v\epsilon)$, as a replacement of the feed volume, Q. The concentration, C, will be a function of v and $(Q - v\epsilon)$. From the definition of a total differential

$$dC = \left(\frac{\partial C}{\partial v}\right)_{Q-v\epsilon} dv + \left(\frac{\partial C}{\partial(Q - v\epsilon)}\right)_v d(Q - v\epsilon) \tag{7}$$

and

$$\left(\frac{\partial C}{\partial v}\right)_Q = \left(\frac{\partial C}{\partial v}\right)_{Q-v\epsilon} - \epsilon \left(\frac{\partial C}{\partial Q}\right)_v \tag{8}$$

Substitution of eq. (8) into eq. (6) results in

$$\left(\frac{\partial C}{\partial v}\right)_{Q-v\epsilon} = - \left(\frac{\partial n}{\partial Q}\right)_v \tag{9}$$

Equations (2), (3), and (9) can be dimensionlessized by first considering the following dimensionless parameters:

$R = r/r_e$ dimensionless pellet radius

$V = v/v_t$ dimensionless bed volume

$X = C/C_o$ dimensionless fluid phase concentration

$Y = \dfrac{n}{\frac{4}{3}\pi r_e^3 b\tau}$ dimensionless reacted phase content in pellet

$Z = \dfrac{3C_o(Q-v\epsilon)}{4\pi r_e^3 b\tau v}$ dimensionless throughput parameter

where,

C_o = inlet gas-phase concentration of species of interest, g-moles/cm^3

v_t = total volume of bed, cm^3

Using these dimensionless expressions, eqs. (9), (2), and (3) become

$$\left(\frac{\partial X}{\partial V}\right)_{ZV} = - \left(\frac{\partial Y}{\partial ZV}\right)_V \tag{10}$$

$$\left(\frac{\partial Y}{\partial ZV}\right)_V = \frac{kav_t X}{F}\left[1 - \frac{ka(1-R_i)}{4\pi\alpha D r_e R_i \tau + ka(1-R_i)}\right] \tag{11}$$

$$\left(\frac{\partial R_i}{\partial XV}\right)_V = - \frac{1}{3R_i^2}\left(\frac{\partial Y}{\partial ZV}\right)_V \tag{12}$$

The group, $(kav_t)/F$, from eq. (11) is also dimensionless. Utilizing this grouping and further defining the following

$K_E = \dfrac{kav_t}{F}$ dimensionless external mass transport property

$$K_I = \frac{4\pi\alpha D\tau r_e v_t}{F} \text{ dimensionless internal mass transport property}$$

Equation (11) can be written

$$\left(\frac{\partial Y}{\partial ZV}\right)_V = K_E X \left[1 - \frac{K_E(1 - R_i)}{K_I R_i + K_E(1 - R_i)}\right] \tag{13}$$

Equations (10), (12), and (13) are the three dimensionless differential equations which completely describe the reacting system of a fluid species in a flowing fluid with a fixed bed of solids and with the assumed mechanisms. The two parameters, K_E and K_I, represent the mass transport properties of the fluid species.

These equations are solvable by a finite difference technique with a digital computer.

2.2 Kinetics of the Co-sorption of H_2O and CO_2 by Type 5-A Molecular Sieves

The experimental data from kinetic tests of the co-sorption of H_2O and CO_2 from flowing streams of He by fixed beds of type 5-A Molecular Sieves is being correlated. An attempt is being made to fit the data to a kinetic model of mass transport of the H_2O and CO_2 from the bulk gas stream to a sorption site controlling the rate of sorption. It is further assumed that the sorbed H_2O irreversibly replaces sorbed CO_2 when both H_2O and CO_2 are competing for sorption sites.

An attempt will be made to use the approximate solution of Tien and Thodos[3] for a single component sorption (with mass transfer controlling) in which a Freundlich-type sorption isotherm is assumed.

The sorption isotherms of CO_2 and H_2O as obtained from Linde Company data[4,5] can be approximated by the following Freundlich-type equations:

For H_2O

$$q_{H_2O} = 0.0535 \; c_{H_2O}^{0.1} \tag{1}$$

For CO_2

$$q_{CO_2} = 0.173 \; c_{CO_2}^{0.3} \tag{2}$$

where

   q = sorption capacity of Molecular Sieves, g-moles/cc

c_{H_2O}, c_{CO_2} = gas-phase concentration of H_2O and CO_2, g-moles/cc

The range of gas-phase contaminant concentration considered is 0.054×10^{-8} to 1.35×10^{-8} g-moles/cc (0.1 to 25 mm Hg gas pressure). In this range, the H_2O sorption capacity is approximated to $\pm 0.05 \times 10^{-2}$ g-moles/cc and the CO_2 sorption capacity is approximated to $\pm 0.10 \times 10^{-3}$ g-moles/cc by eqs. (1) and (2)(Figure 2.1).

References

1. Unit Operations Monthly Progress Report, May 1960, ORNL CF 60-5-58.

2. J. Vermeulen, Advances in Chemical Engineering, Vol II, p. 148-205, New York, Academic Press (1958).

3. Chi Tien and G. Thodos, A.I.Ch.E.J., 5, p.373 (1959).

4. Linde Company, "Molecular Sieves for Selective Adsorption - Water Data Sheets," Form 9690-C (1957).

5. Linde Company, "Molecular Sieves for Selective Adsorption - Non-Hydrocarbon Materials Data Sheets," Form 9691-E (1959).
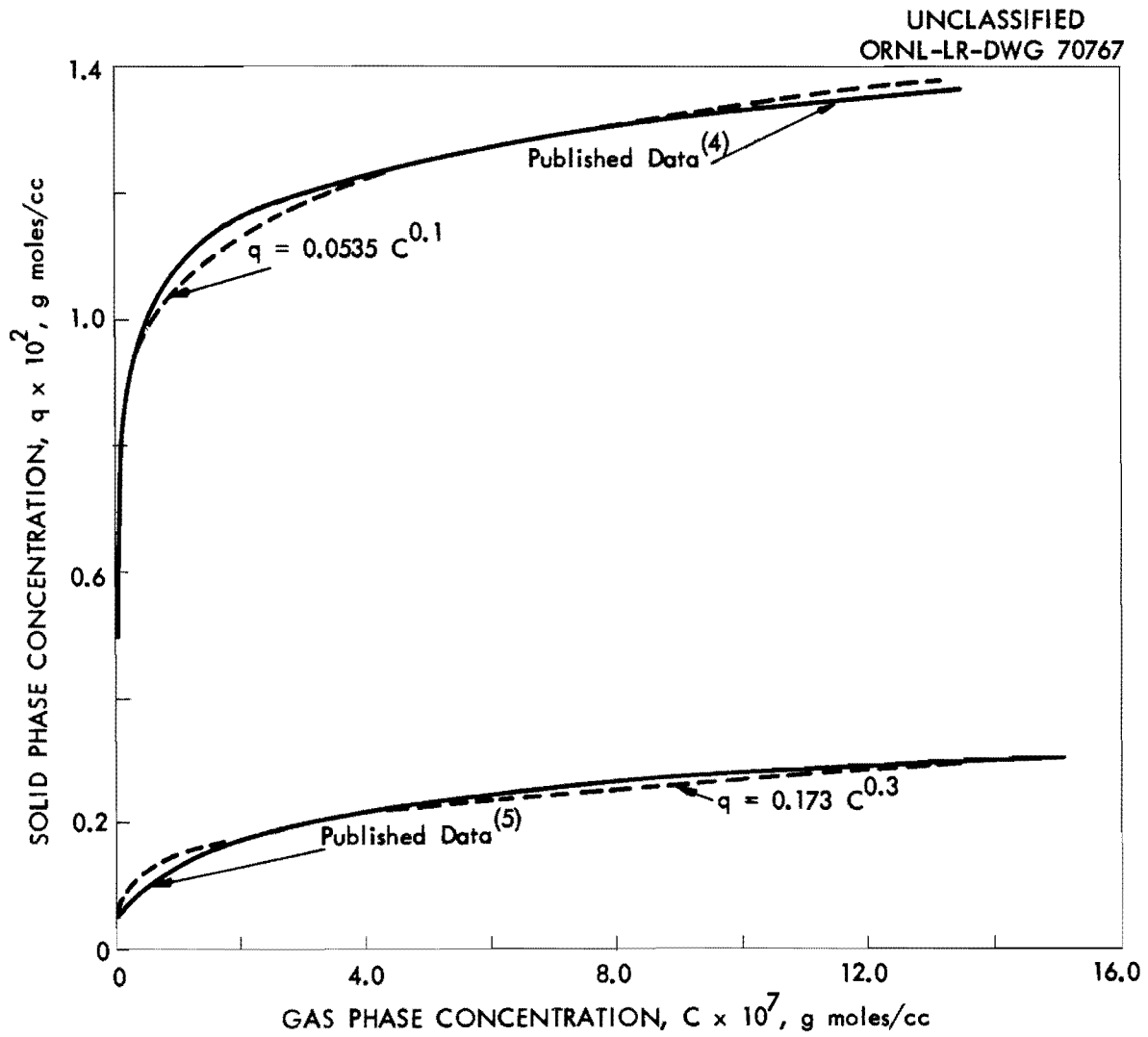
Fig. 2.1.   Sorption isotherms of H_2O and CO_2 on type 5-A molecular sieves at 25°C.

3.0 POWER REACTOR FUEL PROCESSING

C. D. Watson

3.1 Transuranics - Material Evaluation - G. A. West

Plastic materials of construction and protective coatings are under-going radiation damage tests by exposing specimens to a gamma intensity of 1.2×10^6 rad/hr at 40 to 45°C in a cobalt 60 source. Two materials evaluated by bend and visual tests failed at 5×10^7 rad, (1) Penton tubing and sheet material, a chlorinated polyether, Hercules Powder Co., and (2) Armalon gasket material, a tetrafluoroethylene coated glass fabric. The radiation tests will continue on other materials and coatings until failure or until a total exposure of 10^{10} rad is reached. Prospects for developing a smooth continuous floor continues to be poor.

3.2 Mechanical Dejacketing of SRE Core I Fuel - G. A. West

Dejacketed SRE Core I uranium fuel slugs (2.7% enriched, 0.75 in. o.d. x 6 in. long) which were recanned in aluminum have been transferred to the Savannah River Plant for recovery of uranium and plutonium. A total of ~1925 kg of uranium in 2,155 irradiated and 168 unirradiated uranium slugs used in shakedown tests, were transferred in 23 different shipments. This completes the study on SRE Core I fuel. Developmental work will be continued, however, on NaK and Na bonded type fuels to determine the feasibility of other processing methods. Processing techniques which will treat damaged fuel elements more successfully than the hydraulic methods used on Core I such as a chop and leach or roll expansion method will be evaluated.

3.3 Shear and Leach - B. C. Finney, G. A. West, G. B. Dinsmore, J. C. Rose

A shear and leach program to determine the economic and technological feasibility of leaching the core material (UO_2 or UO_2-ThO_2) from relatively short sections (1-in. long) of fuel elements produced by shearing is continuing. This processing method enjoys the apparent advantage of recovering fissile and fertile material from spent power reactor fuel elements without dissolution of the inert jacketing and end adaptors. These unfueled portions are stored directly in a minimum volume as a solid waste. A "cold" shear and leach complex consisting of a shear, conveyor-feeder, and leacher is being evaluated prior to hot runs.

Installation of the complex is completed including check out of the electrical circuitry for both manual and automatic operation. Complete chemical processing equipment has been installed. Wear studies of the gibs, liners, and stepped blade are still in progress. Operation of the shear, blade wear, feeding of fuel assemblies and holding of the terminal portion continues to be satisfactory. The Squarkeen No. 3 stepped blade has made 4507 cuts of the porcelain filled prototype fuel assemblies.

Particle size measurements were made on porcelain filled ORNL Mark I prototype fuel assemblies* which had been sheared into 1, 3/4, 1/2, and 1/4 in. lengths. Particle size distribution appears to be independent of the brazing method (Microbraz-50 vs Kanigen). The shortest practical length to shear prototype fuel appears to be 1/2 in. since the 1/4 in. sheared pieces were flattened and a significant amount of the ceramic was trapped inside the jacket. For sheared lengths of 1, 3/4, 1/2, and 1/4 in., the fraction of particles < 9520 μ in diameter was 11, 16, 33, and 69%, respectively, and for the total fraction of particles < 44 μ, the amounts were 1.5, 2.4, 4.3, and 5.2%, respectively (Figure 3.1). Particles <2000 μ is predominately porcelain, 85 to 99.6%, in all lengths measured (Table 3.1). The braze metal is present in all particle sizes measured, 9520 to < 44 μ, in the amount of 0.1 to 1.0%. A comparison of the 1 in. lengths from a single cut of 36 tube carburized (1.7-2.7% C) ORNL Mark I assembly with a non-carburized element shows: (a) approximately 35% more porcelain is present at particle diameters between 4760 and 9520 μ due to the embrittlement of the stainless steel, (b) the stainless steel is distributed to smaller diameters in amounts of 26% at 590 to 1190 μ compared to 1.3% for non-carburized 1 in. cut element.

Thirteen ORNL Mark I porcelain filled fuel assemblies were sheared into 1/2, 5/8, 1-1/2 in. sections for future particle size distribution studies.

The void fraction of randomly packed batches of fuel obtained by shearing an 8 in. length of an ORNL Mark I porcelain filled fuel assembly into 1/4, 1/2, 5/8, 3/4, 1, and 1-1/2 in. lengths is 0.42, 0.56, 0.58, 0.57, 0.60, and 0.56; respectively (Figure 3.2). There is only a slight difference in the void fraction of sections 1/2 in. and larger (0.56-0.60). The somewhat greater difference in the 1/4 in. sections (0.42) is attributed to virtually complete dislodgement of the porcelain and flattening of the tubing of 1/4 in. sections whereas the other lengths remain essentially right cylinders.

Three porcelain filled Mark I fuel assemblies fabricated with 1/8 in. thick stainless steel tube sheets located 1/2 in. from each end of the assemblies were sheared into 1/2 in. sections. In two of six cuts through tube sheets, a chunk of assembly was produced containing 7 sections of tubing and a triangular shaped piece of tube sheet with ~2 in. sides; and a chunk containing 25 tubing sections attached to a piece of tube sheet. The larger chunk jammed between the adjustable stop and inner gag on the reverse stroke of the ram resulting in some deformation of the adjustable stop (Figure 3.3). The results of the cuts made through the tube sheet sections indicate that it may not be advisable to shear assemblies containing tube sheets in the 250 ton prototype shear.

---

*36 type 304 stainless steel tubes, 1/2 in. o.d., 20 mil thick x 72 in. long, with 1/4 in. o.d. x 1 in. long spacer ferrules brazed on with Microbraz-50 or Kanigen.

Shearing Conditions:

(1) Horizontal actuated ORNL
250 ton shear, stepped blade,
Operated at 1.22 in./sec and
~4.2 cuts/min

(2) ORNL-Mark I fuel: square
bundle of 36 tubes, 1/2" OD,
72" long, with 1/4" OD x 1"
long spacer ferrules at ~12"
intervals. Tubes filled with
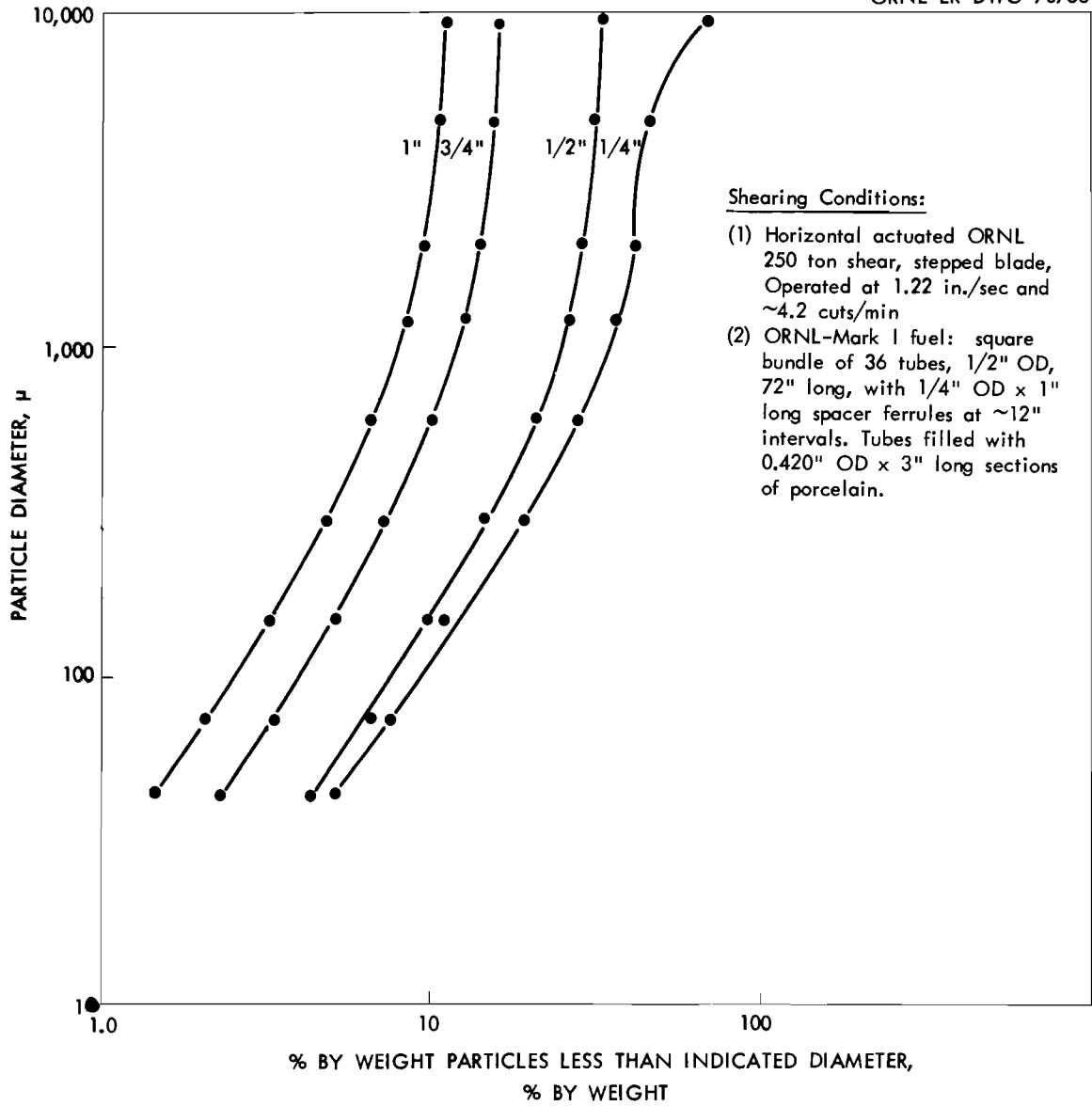0.420" OD x 3" long sections
of porcelain.

Fig. 3.1. Particles dislodged from shearing of ORNL-Mark I fuel into 1", 3/4", 1/2", and 1/4" lengths.

Table 3.1. Porcelain, Stainless Steel, and Braze Metal Distribution, Wt %, at Various Particle Diameters Produced from Shearing of ORNL Mark I Fuel into 1, 3/4, 1/2, and 1/4 in. Lengths

Conditions: (1) Horizontal actuated ORNL 250 ton shear with a stepped blade operated at 1.22 in./sec and ~4.2 cuts/min.
(2) ORNL Mark I fuel is a 3-5/8 in. square bundle of 36 type 304 stainless steel tubes, 1/2 in. o.d. x 72 in. long with 1/4 in. x 1 in. long spacer ferrules brazed on at ~12 in. intervals. The tubes are filled with ~1600 g of porcelain sections 0.42 in. o.d. x 3 in. long.

Particle Diameter	1 in. cut			(Carburized)* 1 in. cut		3/4 in. cut			1/2 in. cut			1/4 in. cut		
	Porcelain	Stainless Steel	Braze	Porcelain	Stainless Steel	Porcelain	Stainless Steel	Braze	Porcelain	Stainless Steel	Braze	Porcelain	Stainless Steel	Braze
μ	%	%	%	%	%	%	%	%	%	%	%	%	%	%
9519 to 4760	31.0	68.0	1.0	48.6	51.4	9.0	90.75	0.25	59.0	40.7	0.3	9.2	90.6	0.2
4759 to 2000	49.6	49.8	0.6	43.6	56.4	60.0	39.5	0.5	68.0	31.4	0.6	29.8	69.7	0.5
1999 to 1190	85.0	14.6	0.4	62.2	37.8	97.1	2.7	0.2	95.0	4.8	0.2	90.2	9.7	0.1
1189 to 590	98.2	1.3	0.5	74.1	25.9	99.0	0.9	0.1	98.0	1.9	0.1	97.7	2.1	0.2
589 to 297	99.1	0.4	0.5	87.0	13.0	99.4	0.4	0.2	99.2	0.6	0.2	98.9	0.8	0.3
296 to 149	99.3	0.3	0.4	89.7	10.3	99.4	0.3	0.3	99.4	0.4	0.2	98.8	0.7	0.5
148 to 74	99.2	0.3	0.5	93.0	7.0	99.3	0.3	0.4	99.5	0.3	0.2	98.6	0.6	0.8
73 to 44	99.2	0.4	0.4	92.4	7.6	99.4	0.2	0.4	99.5	0.3	0.2	98.5	0.5	1.0
< 44	98.6	1.0	0.4	95.2	4.8	99.0	0.7	0.3	99.6	0.2	0.2	98.2	0.8	1.0

*Distribution of single cut of carburized (1.7-2.7% C) ORNL Mark I assembly.
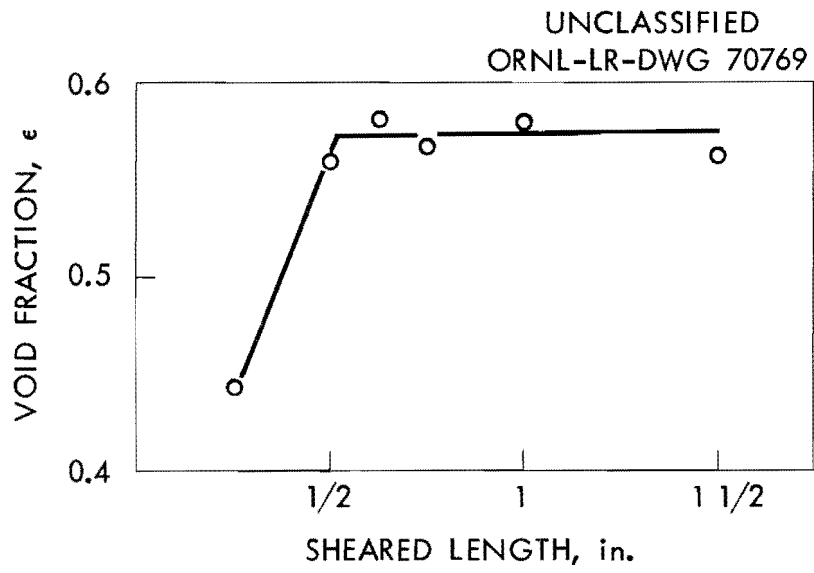
Fig. 3.2. Void fraction as a function of sheared length for porcelain filled ORNL-Mark I prototype fuel assemblies.
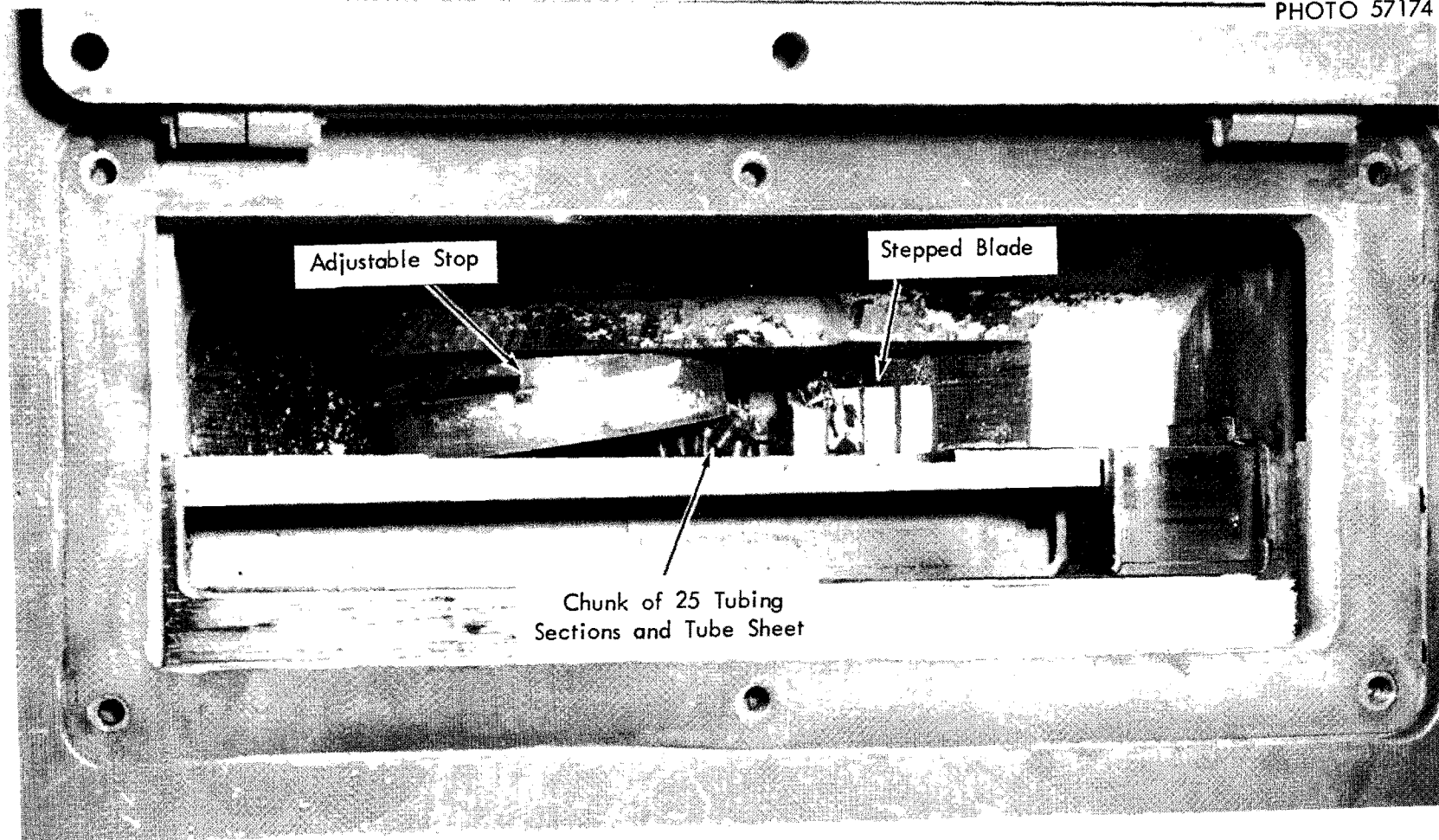
Fig. 3.3. Chunk of 25 tubing sections and tube sheet (porcelain-filled ORNL Mark I) jammed between adjustable stop and inner gag.

Three porcelain filled Yankee prototype subassemblies were sheared into various lengths for particle size determination. The assemblies were fed into the shear without difficulty despite projecting side spacer ferrules. Some chunks containing several tubular sections were produced at the ferrules, but this is probably due to the center step of the stepped blade being too wide for the Yankee subassembly.

Power measurements made using a strain gage transducer and Sanborn Recorder indicate that a maximum power of 26.5 hp is required to shear through a row of ferrules of a porcelain filled ORNL Mark I prototype fuel assembly with Nicrobraz-50 as the bonding agent (Figure 3.4).

Shearing Speed: 1.22 inches/sec
Total Work: 24669 ft-lbs
Horsepower (avg.): 6.26
Max. Pressure: 480 psig
Avg. Pressure: 116 psig
Friction Work: 10885 ft-lbs
Shearing Work: 13784 ft-lbs
Horsepower (loss to fraction): 2.76 HP
Max. Horsepower: 26.5 HP

Fig. 3.4. Hydraulic pressure as a function of ram travel for shearing through a row of ferrules of a porcelain filled Nicro Braz 50 ORNL-Mark I prototype fuel assembly using the 250 ton prototype shear.

4.0 SOLVENT EXTRACTION STUDIES

A. D. Ryon

The flow capacities of nozzle plate columns operated under dilute purex flowsheet conditions are reported this month.
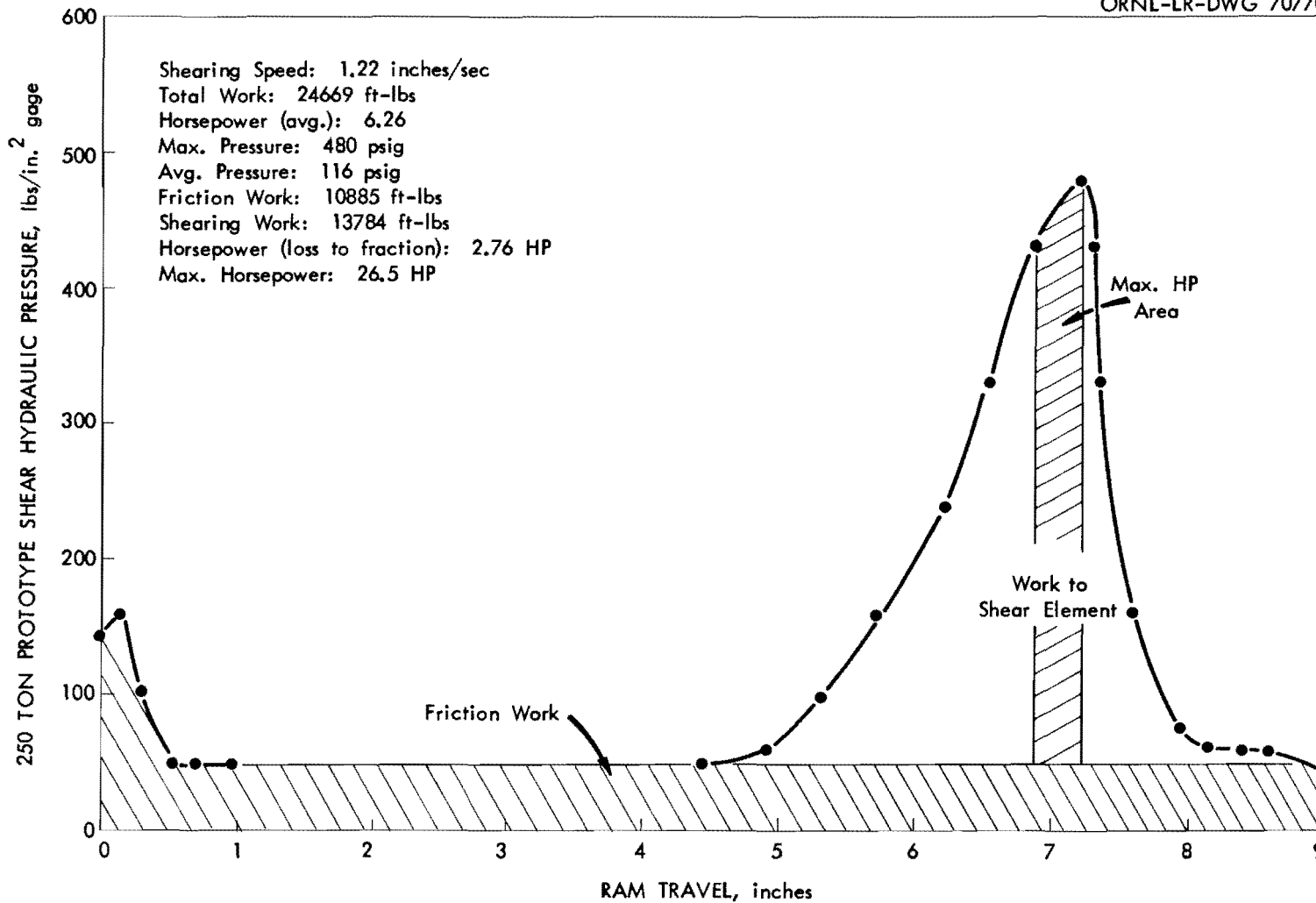
4.1 Dilute Purex Flowsheet Studies - Flow Capacity of Nozzle Plate Pulse Columns - R. S. Lowrie, A. Faure
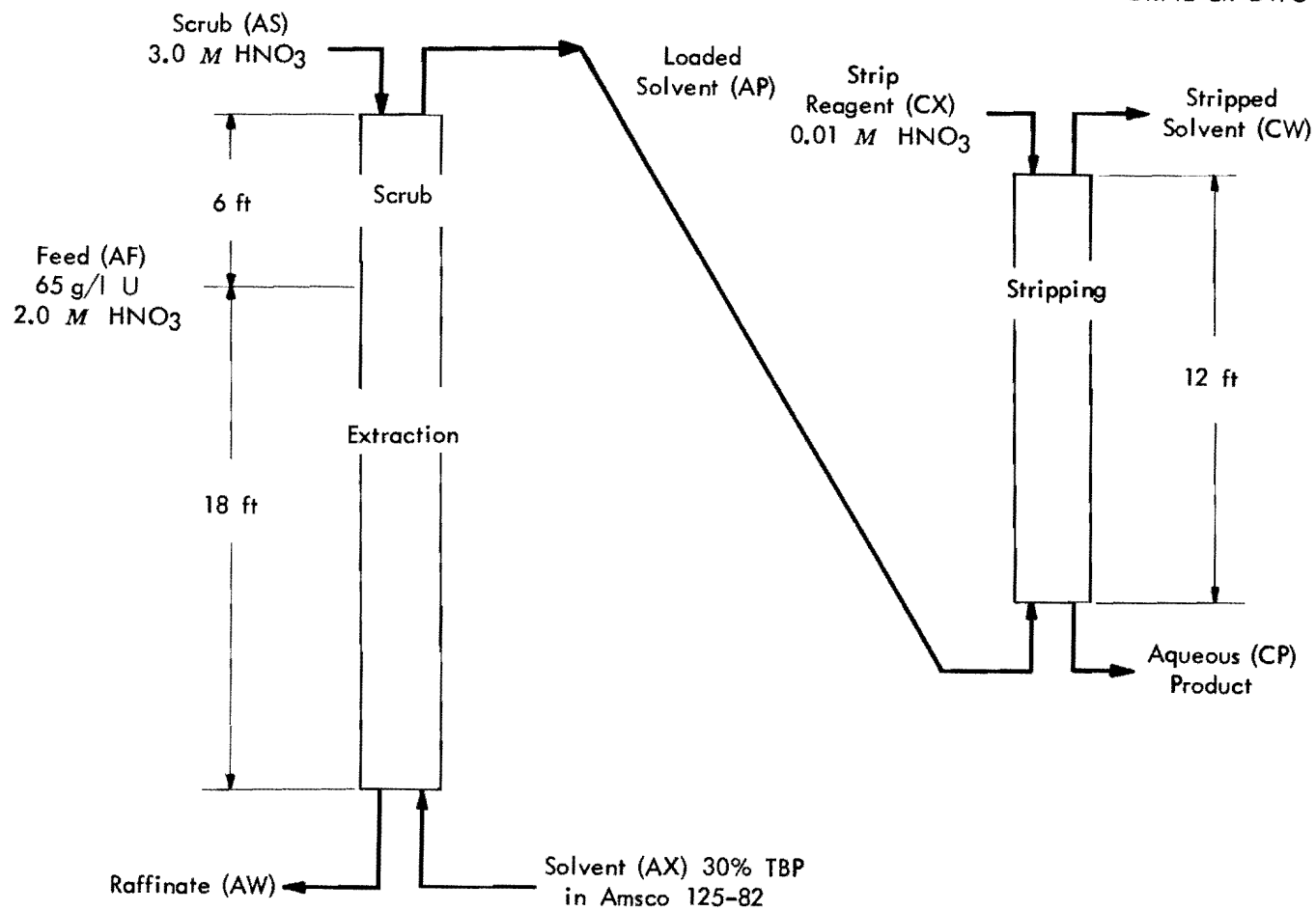
Studies were made to determine the flow capacity of nozzle plate pulse columns under dilute purex flowsheet conditions. This flowsheet (Figure 4.1) was designed to use the first cycle aqueous uranium product with only minor adjustment to feed the second uranium cycle, thus eliminating the need for an intercycle evaporator in the feed adjustment step. The main differences from the standard purex flowsheet were the uranium concentration in the feed (65 g/liter vs 320 g/liter) and the solvent to feed flow ratio which was set to give the same uranium concentration in the loaded solvent (AP) stream. The solvent was 30% TBP in Amsco 125-82 and the loaded solvent was stripped with 0.01 $\underline{M}$ nitric acid. Composition and physical properties of the test solutions are shown in Table 4.1.

Two 24 ft test columns, one equipped with nozzle plates having 0.125 in. dia nozzle and 10% free area, the other equipped with nozzle plates having the same size nozzles but 23% free area, were used either as compound extraction-scrub or simple extraction columns in the flooding tests. The nozzles were oriented down for solvent continuous operation (bottom interface). Flooding always occurred at the feed point and the flow capacity reported is the total flow in the extraction section. The nozzle plates (0.125 in. dia nozzles, 10% free area) in the 12 ft stripping column were oriented up for aqueous continuous operation (top interface). Flooding occurred at the bottom of the column.

The flow capacity of the compound extraction column using nozzle plates having 23% free area increased from < 420 to 875 gal ft^{-2}hr^{-1} as the pulse frequency dropped from 70 to 35 cpm (Table 4.2). The flow capacity of the compound extraction-scrub column using 10% free area nozzles was not accurately determined but was < 500 gal ft^{-2}hr^{-1} at 35 cpm or less than half the flow capacity of 1160 gal ft^{-2}hr^{-1} obtained in the same column at 35 cpm under standard purex flowsheet conditions.* The flow capacity of 23% free area nozzle plate column operated as a simple extraction column increased from 680 to 875 gal ft^{-2}hr^{-1} as the pulse frequency decreased from 50 to 35 cpm. Note that at 35 cpm the flow capacity was ~60% of that obtained using the standard purex flowsheet. The flow capacity of the simple extraction 10% free area nozzle plate column increased from 350 to 560 gal ft^{-2}hr^{-1} as the pulse frequency

---

*Standard Purex Flow Ratios

Feed	Scrub	Solvent	Strip
100	66	367	666

Scrub (AS)
3.0 M HNO$_3$

Loaded
Solvent (AP)

Strip
Reagent (CX)
0.01 M HNO$_3$

Stripped
Solvent (CW)

6 ft

Scrub

Stripping

Feed (AF)
65 g/l U
2.0 M HNO$_3$

12 ft

Extraction

18 ft

Aqueous (CP)
Product

Raffinate (AW)

Solvent (AX) 30% TBP
in Amsco 125-82

Flow Ratios	Feed	Scrub	Solvent	Strip
	100	15	77	140

Fig. 4.1. Dilute purex flowsheet.

Table 4.1. Physical Properties of Test Solutions

Test Solution	U, g/liter	H^+, $\underline{M}$	Density g/cc	Viscosity, centipoise
Feed (AF)	65	2.0	1.16	1.12
Scrub (AS)	0	3.0	1.09	0.97
Solvent (AX)	-	-	0.814	1.63
Raffinate (AW)	0.006	1.9	1.06	1.12
Loaded Solvent (AP)	75.6	0.20	0.934	2.67
Strip Reagent (CX)	-	0.01		
Stripped Solvent (CW)	0.0002	0.02	0.814	1.63
U Product (CP)	38.9	0.112	1.05	0.94

Viscosity and density at 25°C.

Table 4.2. Flooding Rates for Nozzle Plate Columns

Pulse Frequency, cpm	Nozzle Plate Free Area* %	Column Operation	Continuous Phase	Flooding Rate	
				Dilute Purex	Standard Purex
				gal ft⁻²hr⁻¹	
		Extraction Columns			
35	23	Compound	Solvent	875	-
50	23	Compound	Solvent	535	-
70	23	Compound	Solvent	< 420	-
35	23	Simple	Solvent	875	1530
50	23	Simple	Solvent	680	880
35	10	Compound	Solvent	< 500	1160
50	10	Compound	Solvent	< 420	790
35	10	Simple	Solvent	560	-
50	10	Simple	Solvent	350	-
		Stripping Column			
25	10	Simple	Aqueous	1170*	1370
35	10	Simple	Aqueous	840*	1120
50	10	Simple	Aqueous	600*	550

*Nozzles oriented down except in dilute purex stripping column.

Pulse amplitude - 1 in.

decreased from 50 to 35 cpm. Not only was the total flow capacity lower
for the dilute purex flowsheet, but the solvent flow capacity was 30 to
40% of the flow capacity for standard purex flowsheet. The two flowsheets
can be directly compared, because the uranium concentration in the loaded
solvent (AP) stream was the same.

Flow capacity of the stripping columns with 10% free area nozzle plates
oriented up increased from 600 to 1170 gal ft^{-2}hr^{-1} as pulse frequency
decreased from 50 to 25 cpm. The flow capacity of the same column with
the nozzles oriented down increased from 550 to 1370 gal ft^{-2}hr^{-1} as pulse
frequency decreased from 50 to 25 cpm. Both columns were operated aqueous
continuous at same flow rates (A/O 1.8/1.0) solvent loading and strip
reagent. Flow capacity was higher with the nozzles oriented downward
at the lower pulse frequencies.

4.2 Column Pressure Tests

The extraction columns were balanced during the flooding tests against
a water purged leg so instrumented that the total column pressure could
be continuously recorded. Generally, a constant column pressure, indicative
of steady state operation, was achieved in 30 min or less. Column pressure
varied less than 1% during the longest experimental run made (1.25 hrs).
A plot of the experimental data (Table 4.3 and Figure 4.2) results in a
family of nearly parallel lines whose slope is dependent on dispersed
phase holdup. The static head for a simple column may be calculated using
the following equation

$$H = h \left[(1 - x) \rho_o + x \rho_a \right]$$

where

H = static head

h = height of nozzle plate section

x = holdup of dispersed phase, %

ρ_o = average density of organic phase

ρ_a = average density of aqueous phase

(For simplicity, the end sections are not considered in the formula since
they are essentially constant values.) The static head was calculated
for 10 and 20% dispersed phase holdups using the AW density (1.06 g/cc)
and fresh solvent density (0.86 g/cc). (These densities were used, since
at steady state operation, most of the change in density of the aqueous
phase and concomitantly of the organic phase, occurs in the top foot of
packed section of the column, so that over most of the column length,
the AW and fresh solvent densities prevail.) A plot of this data gave
a line whose slope was essentially the same as that obtained with the
experimental data. The column pressure of the compound extraction-scrub

Table 4.3. Column Pressure Test Data

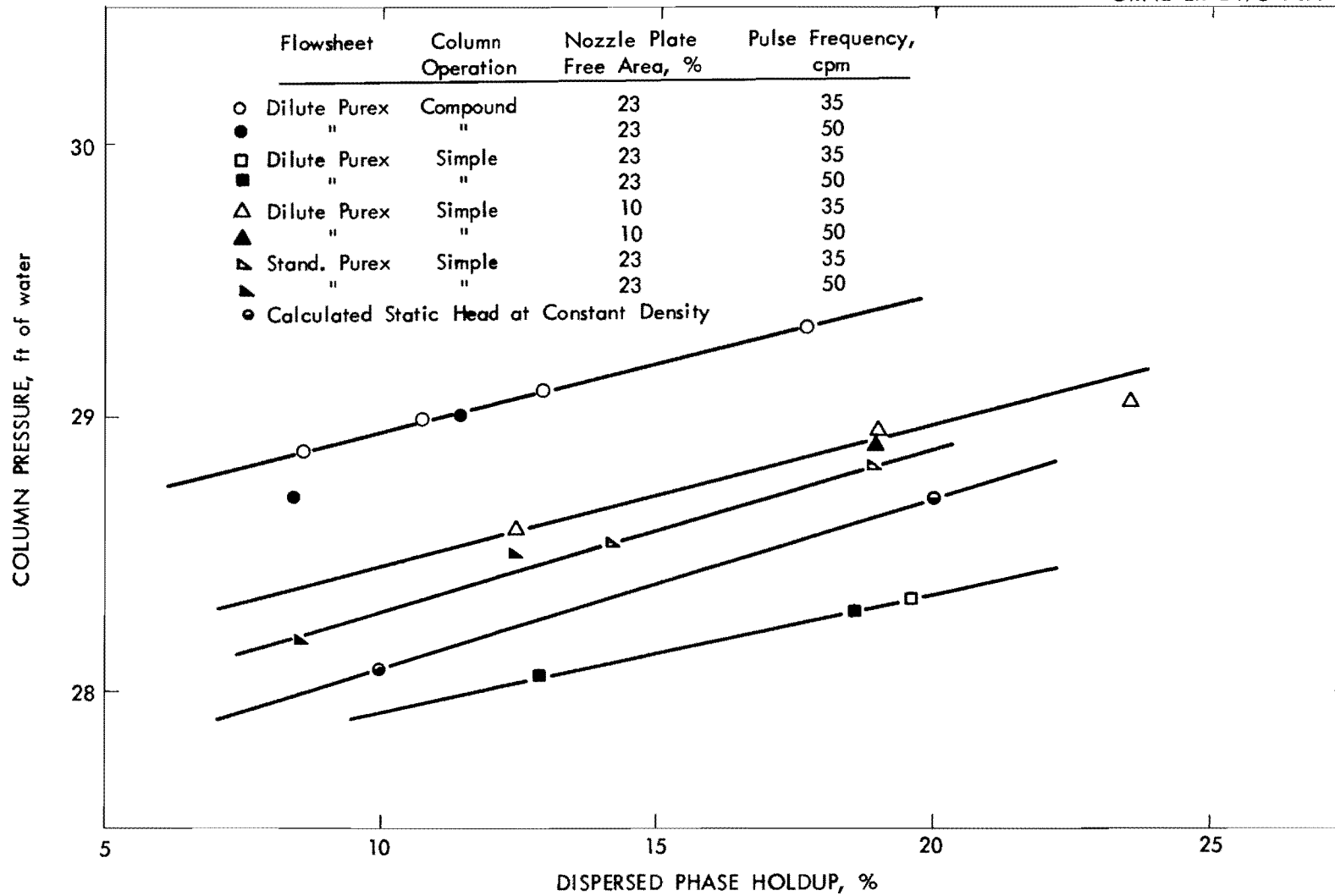| Column Operation	Nozzle Plate Free Area	Pulse Frequency	Dispersed Phase Flow Rate	Dispersed Phase Holdup	Column Head
	%	cpm	gal ft^{-2}hr^{-1}	%	ft of H$_2$O
Dilute Purex Flowsheet					
Compound	23	35	292	8.64	28.87
			365	10.73	29.00
			438	12.96	29.12
			475	17.75	29.33
		50	220	8.44	28.71
			256	11.48	29.00
Simple	23	35	475	19.58	28.33
		50	292	12.80	28.07
			365	18.56	28.54
Simple	10	35	220	12.49	28.58
			256	18.90	28.96
			292	23.63	29.04
		50	183	18.90	28.93
Standard Purex Flowsheet					
Simple	23	35	365	14.18	28.54
			438	18.90	28.83
		50	220	8.51	28.17
			256	12.49	28.50

Fig. 4.2.   Effect of holdup on column pressure.

column was higher than the simple column since the density of the solvent in the 8 ft scrub section approximates that of the loaded solvent (0.94 g/cc).

It has been proposed that column pressure data be used to evaluate the density of the loaded solvent. This is feasible particularly for a simple column if the dispersed phase holdup is known and the aqueous density is held constant (at the AW value). However, if the dispersed phase holdup is not known; varying the holdup from 10 to 20% would introduce a 3% error in the calculated solvent density due to the column pressure-dispersed phase holdup dependency shown in Figure 4.2.

5.0 THORIUM UTILIZATION STUDIES

P. A. Haas

The present emphasis of this program is on development of processes to make ThO_2-$U(233)O_2$ fuel elements. Development is being completed of individual steps of the Sol-Gel Process. Consistent operation of the 14 in. dia rotary denitrator to produce acceptable product was demonstrated. Acceptable calcination and reduction equipment and procedures were developed. Final selection of the detailed procedures for preparation of the thoria-urania sols from denitrator product and $UO_2(NO_3)_2$ solutions is in progress. Sampling and analytical requirements for verifying product compositions are being investigated. Design of the Kilorod facility is being critically reviewed with respect to applying the engineering development experiences. Irradiation of fuel specimens is continuing.

5.1 Irradiation Testing - S. D. Clinton

Eight fuel pins, 11 in. long, 5/16 in. o.d., containing sol-gel ThO_2-UO_2 have performed satisfactorily in the NRX reactor during the past 12 month period beginning on April 6, 1961. Each specimen contains mixtures of three different particle size fractions of ThO_2-UO_2 vibratorily compacted to bulk densities between 8.6 and 8.7 g/cc, and the fully-enriched uranium content of the fuel is 4.2 to 4.4 wt %. The peak cladding heat flux was estimated at 300,000 Btu/hr ft^2 at the start of the irradiation, however, the present peak cladding heat flux is approximately 220,000 Btu/hr ft^2. The PRFR irradiation holder is scheduled for removal during May 1962, at which time the sol-gel fuel pins will have accumulated between 10,000 and 17,000 megawatt days/ton of Th depending on the specimen location in the holder. The replacement PRFR holder will contain six fuel pins, 39 in. long, containing sol-gel ThO_2-UO_2 (5.0 wt % fully-enriched U) pneumatically vibrated to a bulk density of 8.8 g/cc, and three fuel pins, 11 in. long, containing ThO_2-PuO_2 (4.0 wt % Pu-239) "hand loaded" to a bulk density of 7.5 g/cc. A peak cladding heat flux of 350,000 Btu/hr ft^2 is predicted for these specimens.

Four specimens, 22 in. long, containing arc-fused and sol-gel ThO_2-UO_2 were inserted in the NRX reactor on November 20, 1961; and were removed on February 16, 1962, due to a full-scale reading (50 mr/hr) on a gaseous fission product monitor. Visual examination of the removed capsules, which had accumulated between 3,000 and 5,000 megawatt days/ton Th, indicated a corroded area located at 6 to 8 in. from the end of specimen C-3. The failed rod contained a ThO_2-UO_2 preparation (sol-gel C) which was not prepared by the "standard sol-gel process." Although the oxide was known to have inferior properties (vibrated to a maximum bulk density of 8.3 g/cc), failure was probably due to bowing. In order to minimize the probability of bowing failures for the 39 in. long specimens, a 35 mil dia spring wire was wound around the clad with a 2 in. pitch and welded to the end plugs.

Seven capsules, 11 in. long, were inserted in the MTR between October 16 and December 18, 1961. These specimens contain sol-gel and arc-fused ThO_2-UO_2 (approximately 4.0 wt % fully-enriched uranium) pneumatically vibrated to bulk densities between 8.6 and 8.7 g/cc. At the start of the irradiation the peak cladding heat flux was estimated at 600,000 Btu/hr ft^2 with a peak unperturbed thermal neutron flux of 1×10^{14}. On April 2, 1962, two of these capsules were removed (12,000 to 14,000 megawatt days/ton Th) for normal post-irradiation examination. Due to the burn-up of U-235 the remaining five capsules are scheduled for a 50% increase in unperturbed thermal neutron flux during May 1962 and should remain at this flux for at least 12 months.

Two capsules each containing sol-gel ThO_2-UO_2 (2.5 wt % fully-enriched uranium) and a central thermocouple, were inserted in the ORR pool-side facility (03-5 and 06-5) at an unperturbed thermal neutron flux of 3×10^{13} during January 1962. Each of the capsules was pneumatically vibrated to a bulk density of 8.6 g/cc and designed to operate at 40,000 Btu/hr ft with an active fuel length of 5.5 in. The average cladding temperatures of experiments 03-5 and 06-5 are 1300°F and 1000°F, respectively. During the three months of in-pile operation, the central temperature of 03-5 has decreased steadily from an initial 3600°F to approximately 2800°F. This decrease may be attributed to thermocouple drift, fuel sintering, or a combination of both. The central thermocouple of 06-5 has remained essentially constant at 2700°F. Based on the design heat generation rate, the effective thermal conductivity of the ThO_2-UO_2 (centerline to cladding surface) is in the order of 1.2 to 1.5 Btu/hr ft °F which compares favorably with pelleted fuels. The two capsules are scheduled for removal in July 1962, which corresponds to a burn-up of approximately 5,000 megawatt days/ton Th.

5.2 Thorium Nitrate Denitration Studies - J. W. Snider, R. D. Arthur

Twenty-two runs were made with the 14-in.-dia rotary denitrator producing approximately 325 kg of ThO_2 powders. Nineteen of these were made with a 30 kg charge of $Th(NO_3)_4 \cdot xH_2O$ and three with a 45 kg charge. Fifteen of these runs resulted in ThO_2 products which were free of the undesirable creamy fraction. Twelve of the good runs were made in succession by delaying the steam contact time until the rotating drum temperature reached 180°C. Thorium carry-over into the condenser system averaged 0.89% with a maximum of 1.43% and a minimum of 0.46%.

The operating conditions for these runs are given in Table 5.1. Repeative runs were not made under completely identical conditions although steam flow rates and time at various rates were constant, but the differences are not evident from Table 5.1. For example: Figures 5.1, 5.2, and 5.3 each show two runs made with identical charge weights, and heater and steam control settings versus time. The times required to reach a given temperature under a given steam rate varied along with the shape of the heating profile and the volumes of off-gas condensate in the total condenser. Runs RDB-12, RDB-14, and RDB-31, with products free of the creamy fraction, are represented by broken lines of Figures 5.1, 5.2, and 5.3, respectively. The shape of the heating profile between 250°C

Table 5.1. Rotary Denitrator Run Conditions and Objectives

Charge: 30 kg of $Th(NO_3)_4 \cdot xH_2O$ or as Noted

Run No.	Steam Program Flow Rate, lb/hr	Inlet Temp., °C	No. of min	Percent Thorium Carry-over	Creamy Fraction Absent (i.e. Product Good)	Purpose of Run, Other Conditions and Remarks
RDB-11	34	410	80 + 10*	0.78	No	To duplicate good product of run 10.
	22	360	280			
RDB-12	29	400	78 + 15	0.80	Yes	To duplicate good product of run 10.
	17	340	285			
RDB-13	28	400	112 + 15	0.74	No	To maintain the 30 lb/hr steam rate until reaching the second hold period.
	16	340	249			
RDB-14	45	-	23 + 5	1.06	Yes	To test an initial steam rate of > 40 lb/hr for a short time, then hold the 30 lb/hr rate until after the second hold period.
	28	400	120			
	16	340	218			
RDB-15	41	-	25 + 5	1.08	Yes	To duplicate good product of run 14.
	28	400	113			
	16	340	225			
RDB-16	41	425	35 + 5	0.85	No	To duplicate good product of runs 14 and 15.
	28	400	112			
	16	340	215			
RDB-17	16	340	60 + 5	0.71	No	To utilize a low steam rate for the entire run.
	14	330	240			
RDB-18	45	425	30 + 15	0.48	No	To test an initial steam rate of > 40 lb/hr for a short time, then a low steam rate for the remainder of the run.
	14	330	270			
RDB-19	41	425	90	0.46	No	To use run 18 conditions with the high steam rate prevailing until after the second hold period.
	17	340	125			
RDB-20	19	350	330	0.63	Yes	Steam contact delayed until 180°C skin temperature was reached.
RDB-21	19	350	240	0.46	Yes	To duplicate good product of run 20 and to shorten run time.
RDB-22	19	350	240	0.60	Yes	To duplicate good product of run 21.
RDB-23	19	350	240	0.51	Yes	To duplicate good products of runs 21 and 22.
RDB-24	37	415	103	1.43	Yes	To test the effect of a high steam rate prevailing until after the second hold period with the delayed steam contact time.
	19	350	137			
RD-25	19	350	240	1.03	Yes	To repeat run 21 without the steam gaffle in denitrator.
RDB-26	30	405	142	1.23	Yes	To test the feasibility of a 45 kg $Th(NO_3)_4 \cdot xH_2O$ charge, with the steam contact time delayed.
	19	350	248			
RD-27	19	350	360	1.04	Yes	To extend the time of run 21.
RDB-28	30	405	127 + 15	1.14	Yes	To duplicate run 12 (for a shorter period) and thus confirm effect of early steam contact in producing creamy fraction.
	19	350	158			
RDB-29	41	420	40 + 15	0.97	Yes	To duplicate run 14 to confirm effect of early steam contact in producing creamy fraction.
	28	400	103			
	19	350	202			
RDB-30	30	405	120	0.96	Yes	To determine the effect of a long run time.
	19	350	600			
RDB-31	30	405	120	1.38	Yes	To duplicate run 26.
	19	350	270			
RDB-32	30	405	133	1.17	No	To duplicate run 26.
	19	350	257			

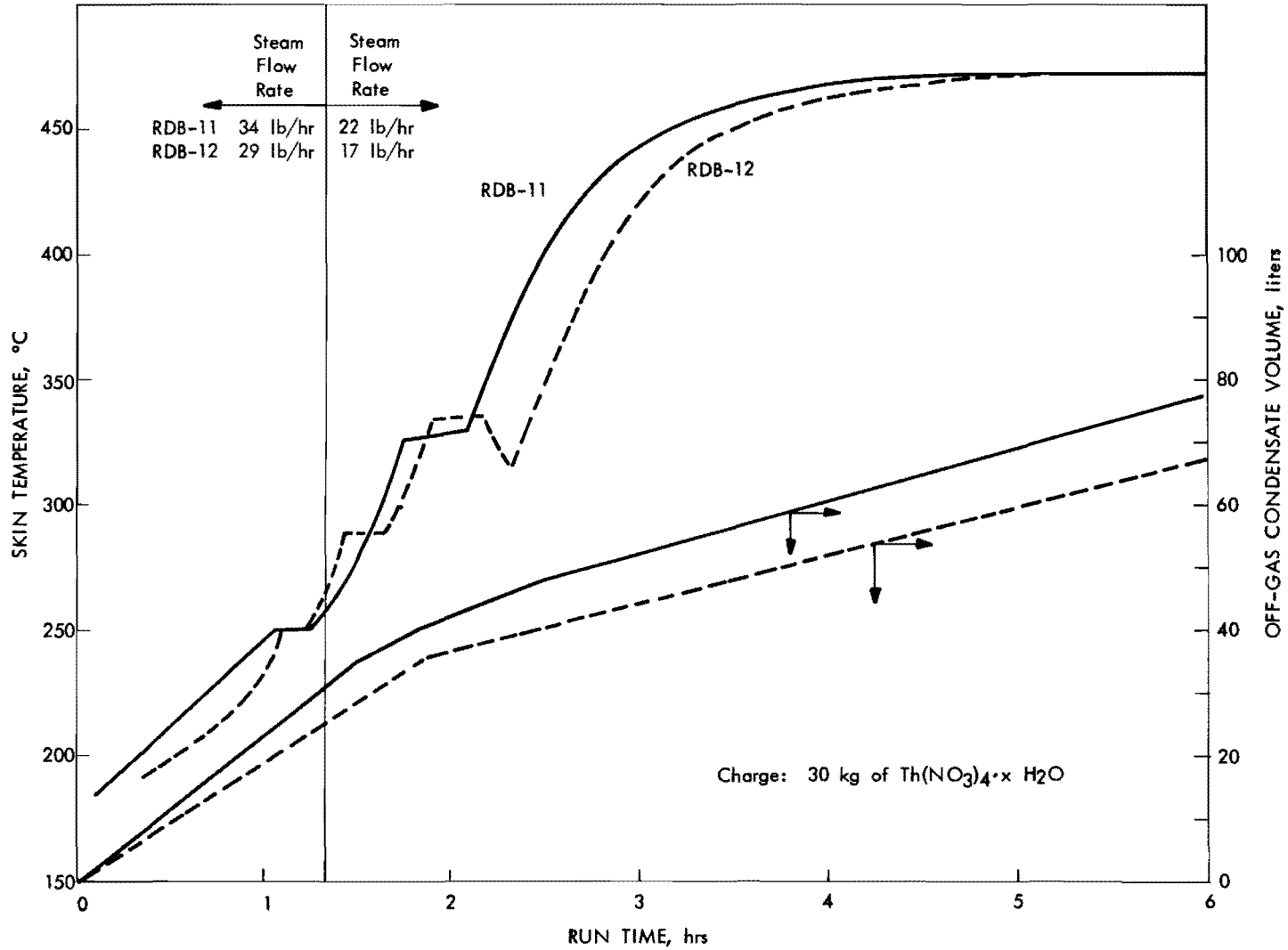*"+ 10" refers to time prior to zero run time.

Fig. 5.1. Rotating drum temperature and condensate volume collected vs. run time for Runs RDB-11 and RDB-12.
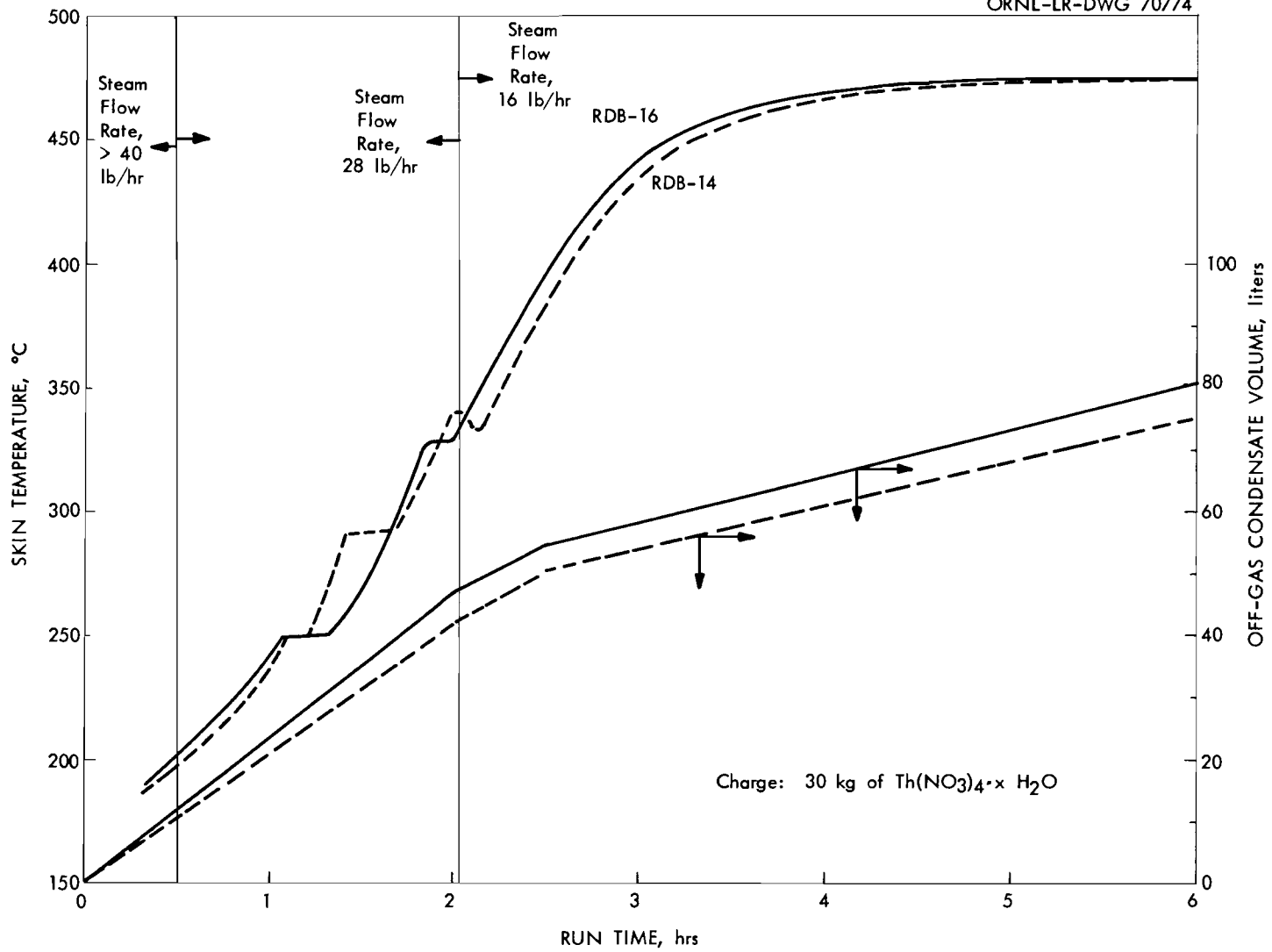
Fig. 5.2. Rotating drum temperature and condensate volume collected vs. run time for Runs RDB-14 and RDB-16.
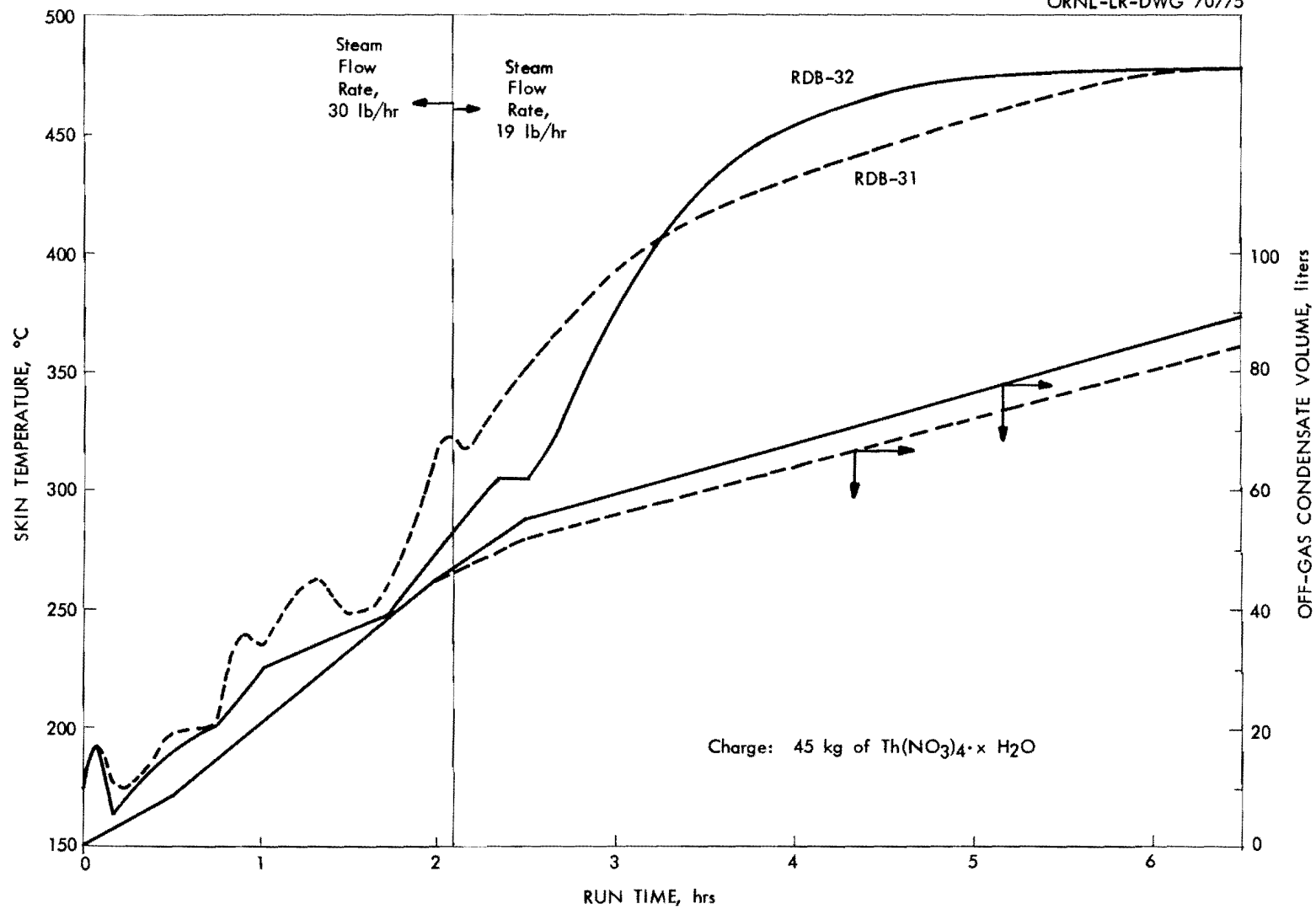
Fig. 5.3. Rotating drum temperature and condensate volume collected vs. run time for Runs RDB-31 and RDB-32.

and 335°C for these good runs is quite different from the runs producing the creamy fraction: runs RDB-11, RDB-16, and RDB-32 represented by solid lines in Figures 5.1, 5.2, and 5.3, respectively.

The runs shown in Figures 5.1 and 5.2 were made with 30 kg charges of Th(NO₃)₄·xH₂O. The heater temperatures reached 500°C at fifteen minutes and controlled at this temperature for the remainder of the run. Three differences were noted between the runs free of the creamy fraction and those containing the creamy fraction. At 290°C an intermediate hold, intermediate between the 250°C and 325°C hold period, period was encountered for the creamy fraction free runs which was not evidenced for the runs containing the creamy fraction. Secondly, upon leaving the 325°C hold period the creamy fraction free runs experienced a decrease in temperature suggesting a much higher endothermic reaction. Thirdly, upon reaching the 250°C hold temperature the creamy fraction runs had evolved 24 or 25 liters of condensate volume and the creamy fraction free runs had evolved < 22-1/2 liters of condensate volume.

There appears to be a relationship between the time required to reach the 250°C hold period, the amount of off-gas condensate volume evolved to this time, and the appearance or absence of the creamy fraction. If all of the 30 kg Th(NO₃)₄·xH₂O runs made with the 14-in.-dia rotary denitrator are examined with this in mind, the results are shown in Table 5.2. For the run conditions of runs 1 through 10, see Unit Operations Section Monthly Progress Report for January 1962, ORNL-TM-150. Empirical criteria which are found to be both necessary and sufficient for the absence of a creamy fraction for the runs listed are that <u>the time required to reach the 250°C hold temperature is ≤ 65 min and that the off-gas collected with total condensation is ≤ 22-1/2 liters (corrected to 30 kg charge)</u>.

The time at which steam contact was made for the runs of Table 5.2 varied from 5 to 25 min after the heaters are turned on. In earlier runs it was discovered that nitrate evolution did not occur until the heater temperature reached 300°C. This was taken as the zero time for all runs except the delayed steam contact runs in which the steam was delayed until the rotating drum temperature reached 180°C. This represents a 15 min delay for the latter type of run, and if this correction is applied to Table 5.2 only one run, RDB-24, would fail the test by 5 min.

The test applies to the three 45 kg Th(NO₃)₄·xH₂O charge runs, RDB-26, RDB-31, and RDB-32; but does not apply to the one small 10.6 kg charge run, RD-6. If the off-gas is proportional according to charge (1.5 kg condensate per kg ThO₂) then the test applies to RD-6. This type of correction holds for the 45 kg charge runs also.

Runs RDB-31 and RDB-32 shown in Figure 5.3 were 45 kg Th(NO₃)₄·xH₂O charge runs. Although the steam contact time was delayed until the rotating drum temperature reached 180°C, run RDB-32 contained the creamy fraction. The rate of condensate collection was the same during the early part of these two runs. Run RDB-32 lagged in temperature and consequently more condensate had been collected when the 250°C hold temperature was reached.

Table 5.2. <u>Times Required to Reach the 250°C Hold Temperature</u>

<u>and the Total Amount of Off-gas Condensate to this Time</u>

<u>for all 30 kg Th(NO$_3$)$_4$·xH$_2$O Runs Made with the</u>

<u>14-in.-dia Rotary Denitrator</u>

Run No.	Time Required to Reach the 250°C Hold Temperature, min	Volume of Off-gas Condensate at the 250°C Hold Time, liters	Creamy Fraction Absent i.e. Good Product
RD-2	80	34	No
RD-3	80	36	No
RD-4	65	27	No
RD-5	65	29	No
RD-7	80	50	No
RD-8	70	29	No
RDB-9	65	16	Yes
RDB-10	65	14	Yes
RDB-11	65	24	No
RDB-12	65	20	Yes
RDB-13	68	20	No
RDB-14	65	22.5	Yes
RDB-15	55	19	Yes
RDB-16	65	25	No
RDB-17	70	12.5	No
RDB-18	70	22.5	No
RDB-19	65	25	No
RDB-20	50	10	Yes
RDB-21	45	9	Yes
RDB-22	45	11	Yes
RDB-23	45	9	Yes
RDB-24	55	19	Yes
RD-25	50	10	Yes
RD-27	50	10	Yes
RDB-28	50	20	Yes
RDB-29	50	21	Yes
RDB-30	50	8	Yes

The value of "x" in the formula $Th(NO_3)_4 \cdot xH_2O$ has varied from 3.90 to 7.11 in feeds used for denitration studies. The value of "x" decreases towards the top of the drums of 92 kg/drum $Th(NO_3)_4 \cdot xH_2O$.

Figure 5.4 is a study of the NO_3 evolution rate as a function of time for a run free of the creamy fraction, RDB-14, and one containing the creamy fraction, RDB-19. There was a large increase in the nitrate evolution rate during the 350°C hold period and the following temperature dip from the creamy fraction free run. This is contrasted to no significant increase in nitrate evolution rate for the creamy fraction run. A second difference was evidenced by the greater amount of nitrate evolved earlier, < 90 min of run time, during the run containing the creamy fraction.

Analysis of the products are shown in Table 5.3. Control of the N/Th mole ratio for runs of 6 hr with steam averaged 0.027 $\pm$ 0.009 and for 4 hr steam contact time followed by air for 1 hr averaged 0.059 $\pm$ 0.005. The runs using 45 kg charges of $Th(NO_3)_4 \cdot xH_2O$ averaged 0.050 $\pm$ 0.006 for 6-1/2 hr of steam contact time. Figure 5.5 is a plot of the $\overline{N}$/Th mole ratio for 30 kg charge runs of $Th(NO_3)_4 \cdot xH_2O$ as a function of run time. The equilibrium N/Th mole ratio, by extrapolation, is ~0.015. Also the large runs do not denitrate to as low a N/Th mole ratio for equal steam contact times.

Run RDB-30 was made to determine the effect of long steam contact times on the denitrated product. The run was made for 5-1/2 hr then allowed to cool overnight and continued the following day. The temperature profile (Figure 5.6) shows the typical hold periods for the denitration as compared to the continuous smooth temperature rise for the second startup. The run time total of 12 hrs, is listed as 10 hr for comparison with other runs in Table 5.3; the 2 hr rise time of the second day was neglected as the assumption was made that denitration would not occur until the previous maximum temperature was approached.

A series of dispersion tests were performed on rotary denitrator products to determine the amount of nitrate which must be added for complete dispersion. This is defined as the nitrate concentration required to retain in suspension > 99.5% of the ThO_2 for a period of 24 hr for a sol column not to exceed 5 in. of height at a concentration of ~2 M ThO_2. The results for some typical products are given in Figure 5.7.

Most rotary denitrator products are completely dispersed by the addition of NO_3 equivalent to a nitrate/thorium mole ratio of 0.07. This value holds for a wide variety of precursor powders. One product, ATC-58, from the agitated trough calciner is included in Figure 5.7. It does not disperse as well as the rotary denitrator products, however, the nitrate/thorium mole ratio which must be added is also 0.07 to achieve maximum dispersion.

Only two of the rotary denitrator products tested failed complete dispersion. They were runs RDB-30, the run that was extended to 10 hrs of steam contact time; and RDB-32, the run containing the creamy fraction.
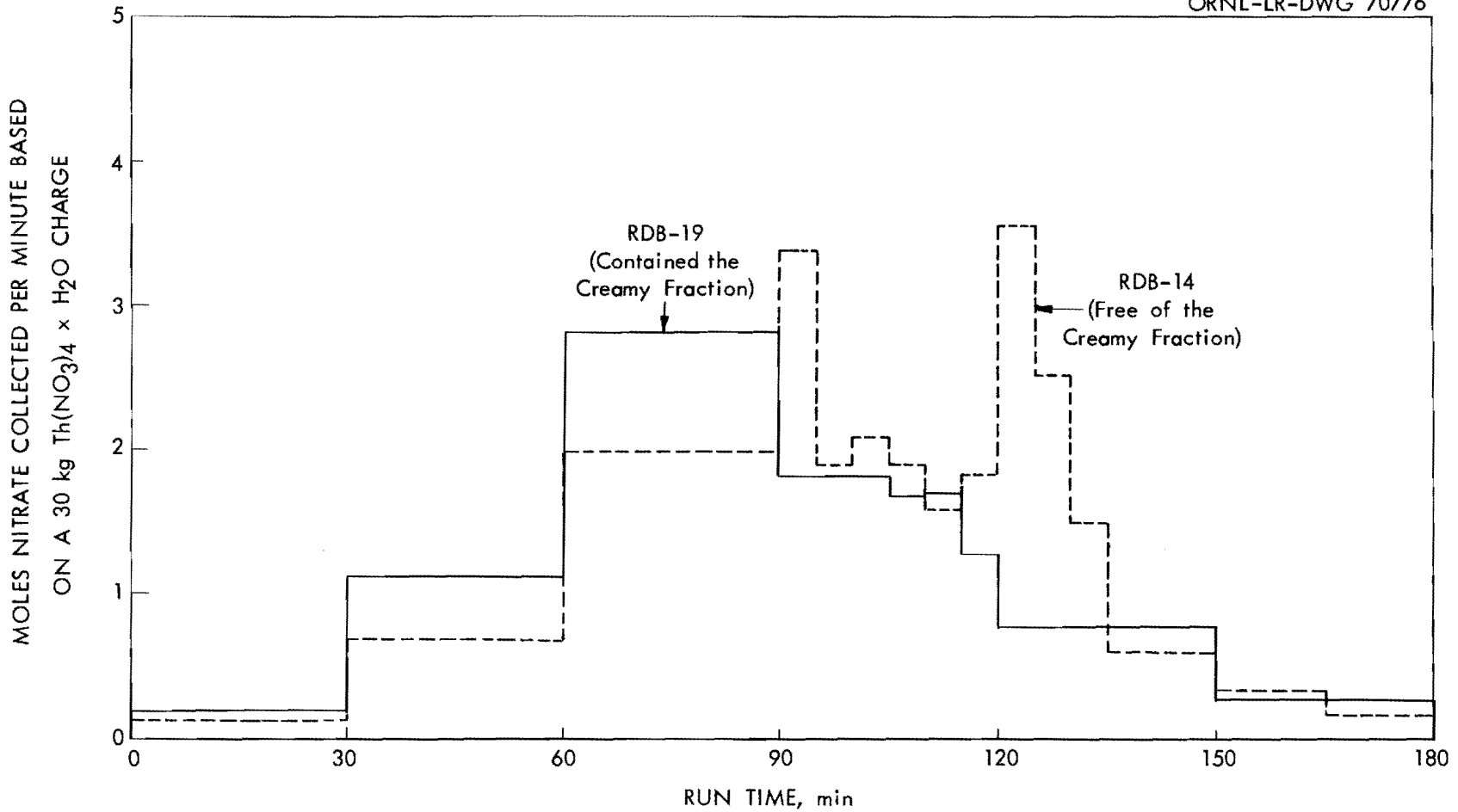
Fig. 5.4. Nitrate evolution rate as a function of run time for a run free of the creamy fraction and for one containing the creamy fraction.

Table 5.3. Analysis of Products Produced in the 14-in.-dia Rotary Denitrator

Run No.	RDB-11[a]	RDB-12	RDB-13	RDB-14	RDB-15	RDB-16	RDB-17	RDB-18	RDB-19	RDB-20	RDB-21	RDB-22
Time in steam, min	360	360	360	360	360	360	300	300	210	330	240	240
Time in air, min	-	-	-	-	-	-	-	-	-	30	60	60
Product weight, kg	14.02	13.96	13.83	14.00	-[c]	-[c]	14.10	13.92	14.13	13.59	13.92	13.70
Thorium carryover, %	0.78	0.80	0.74	1.06	1.08[c]	-[c]	0.71	0.48	0.46	0.63	0.46	0.60
LOI (300-1000°C), %	1.63	1.98	2.16	2.20	2.08	2.14	1.96	1.97	2.45	1.92	2.27	2.54
Nitrogen, %	0.12	0.14	0.15	0.11	0.099	0.091	0.22	0.14	0.41	0.159	0.29	0.33
Thorium, %	86.55	86.53	86.40	85.23	84.96	86.09	84.62	85.34	85.54	86.34	85.38	84.98
N/Th, mole ratio	0.023	0.027	0.029	0.021	0.019	0.018	0.043	0.027	0.079	0.031	0.056	0.064
Crystallite size, A°	77	74	76	72	75	82	76	76	72	69	69	67
Surface area, m²/g	53.8	48.8	49.8	48.3	47.1	51.0	50.0	53.1	50.9	42.2	41.4	39.8
Product free of creamy fraction	No	Yes	No	Yes	Yes	No	No	No	No	Yes	Yes	Yes

	RDB-23[a]	RDB-24	RD-25	RDB-26[b]	RD-27	RDB-28	RDB-29	RDB-30[d]	RDB-31[b]	RDB-32[b]
Time in steam, min	240	240	240	390	360	300	360	600	390	390
Time in air, min	60	60	60	-	-	-	-	-	-	-
Product weight, kg	14.06	13.80	13.54	20.76	13.64	13.88	13.80	13.46	20.77	21.24
Thorium carryover, %	0.51	1.43	1.03	1.23	1.04	1.14	0.97	0.96	1.38	1.17
LOI (300-1000°C), %	2.95	-	-	-	-	-	-	-	-	-
Nitrogen, %	0.32	0.30	0.28	0.22	0.15	0.24	0.14	0.08	0.26	0.29
Thorium, %	84.64	84.94	85.50	85.34	86.11	85.49	86.47	84.25	85.16	85.87
N/Th, mole ratio	0.063	0.059	0.054	0.043	0.028	0.046	0.027	0.016	0.051	0.056
Crystallite size, A°	70	62	68	71	70	64	68	73	66	64
Surface area, m²/g	51.1	45.0	45.3	46.0	50.8	41.6	40.4	38.3	45.5	44.3
Product free of creamy fraction	Yes	Yes	Yes	Yes	Yes	Yes	Yes	Yes	Yes	No

[a] "B" signifies baffled steam inlet.

[b] A 45 kg charge of $Th(NO_3)_4 \cdot xH_2O$ crystals used for these runs.

[c] Product discharged directly in dispersing tank.

[d] 5-1/2 hours of denitration first day; shut down overnight; and 6-1/2 hours of denitration on second day, 2 hours required to reach temperature on the second day not included in run time.
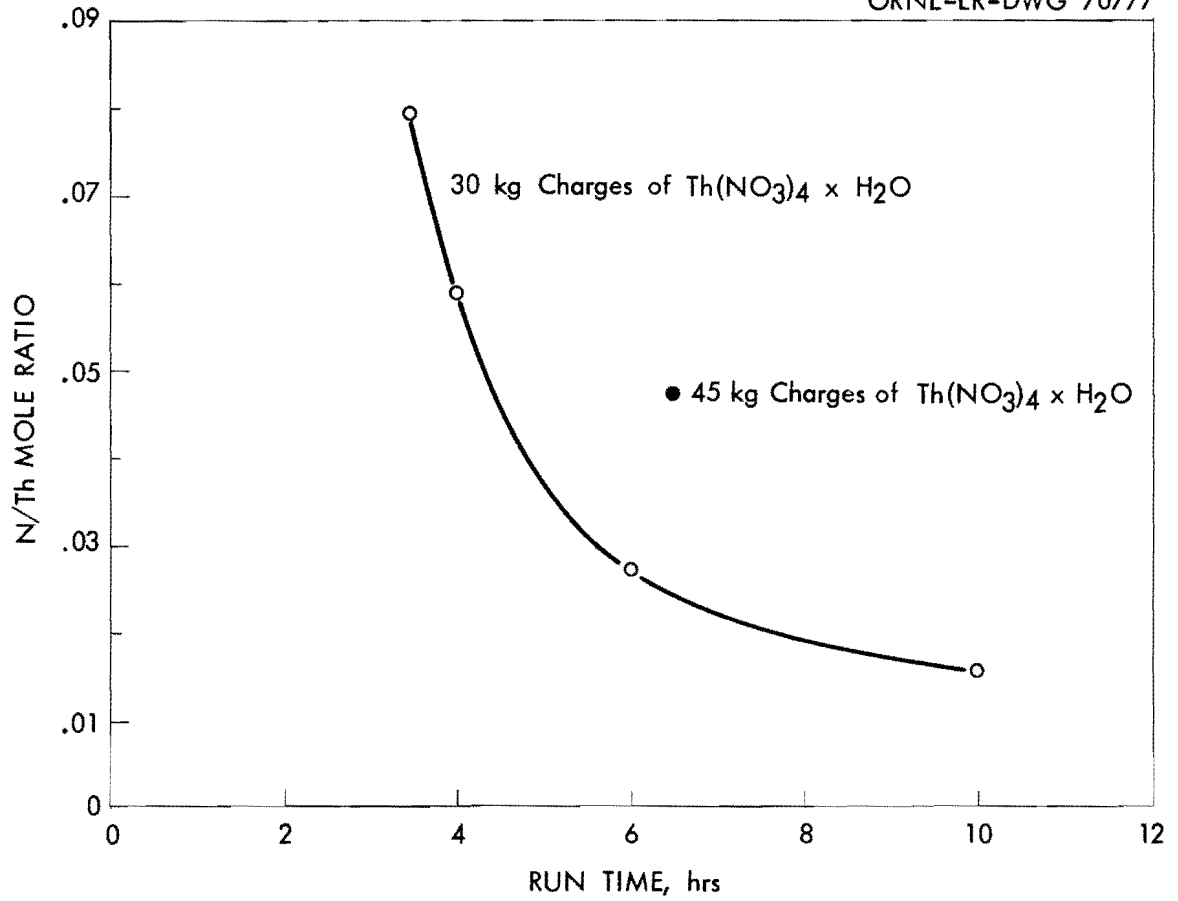
Fig. 5.5. Nitrogen to thorium mole ratio vs run time for 30 kg charges of $Th(NO_3)_4 \times H_2O$.
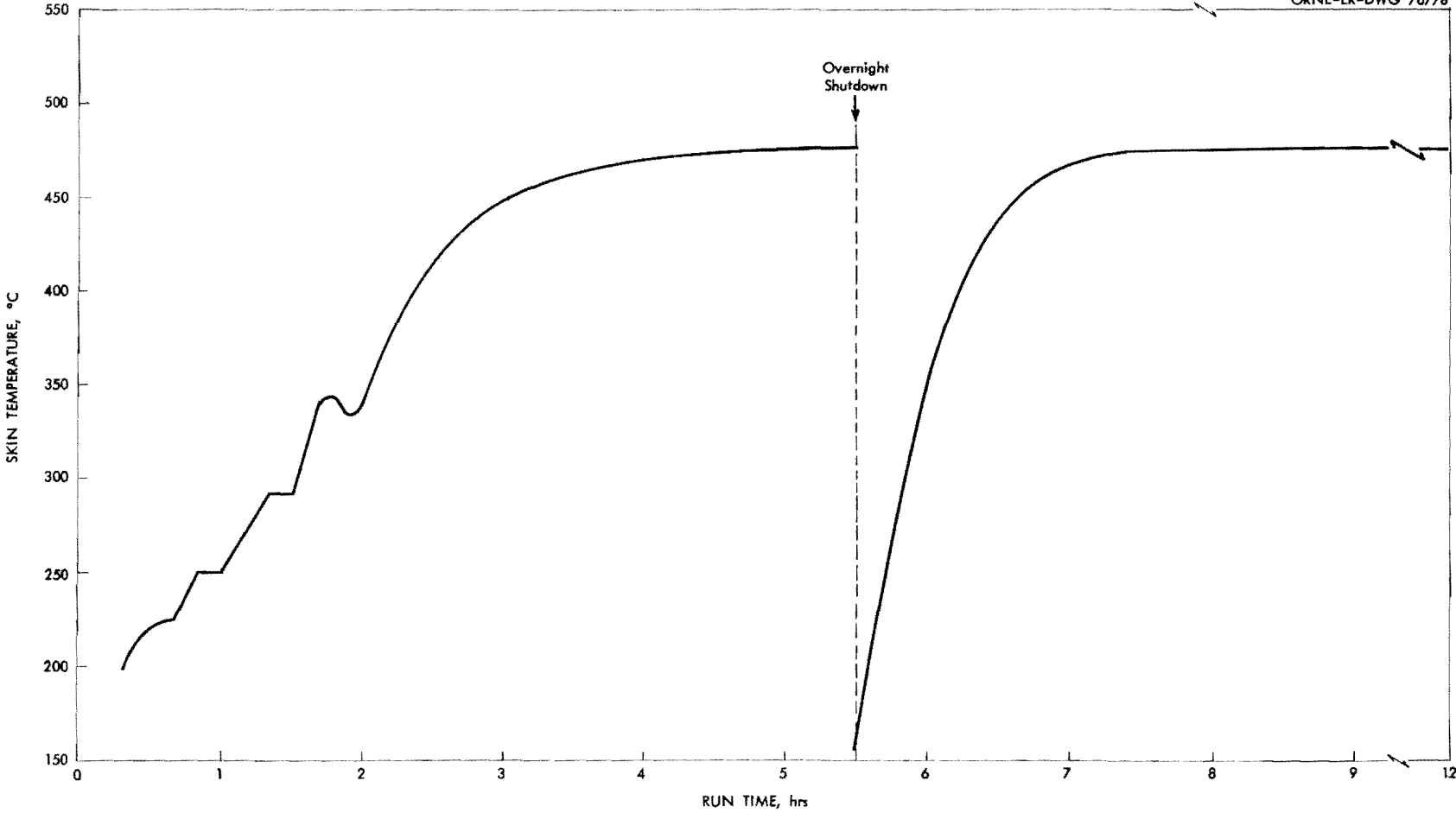
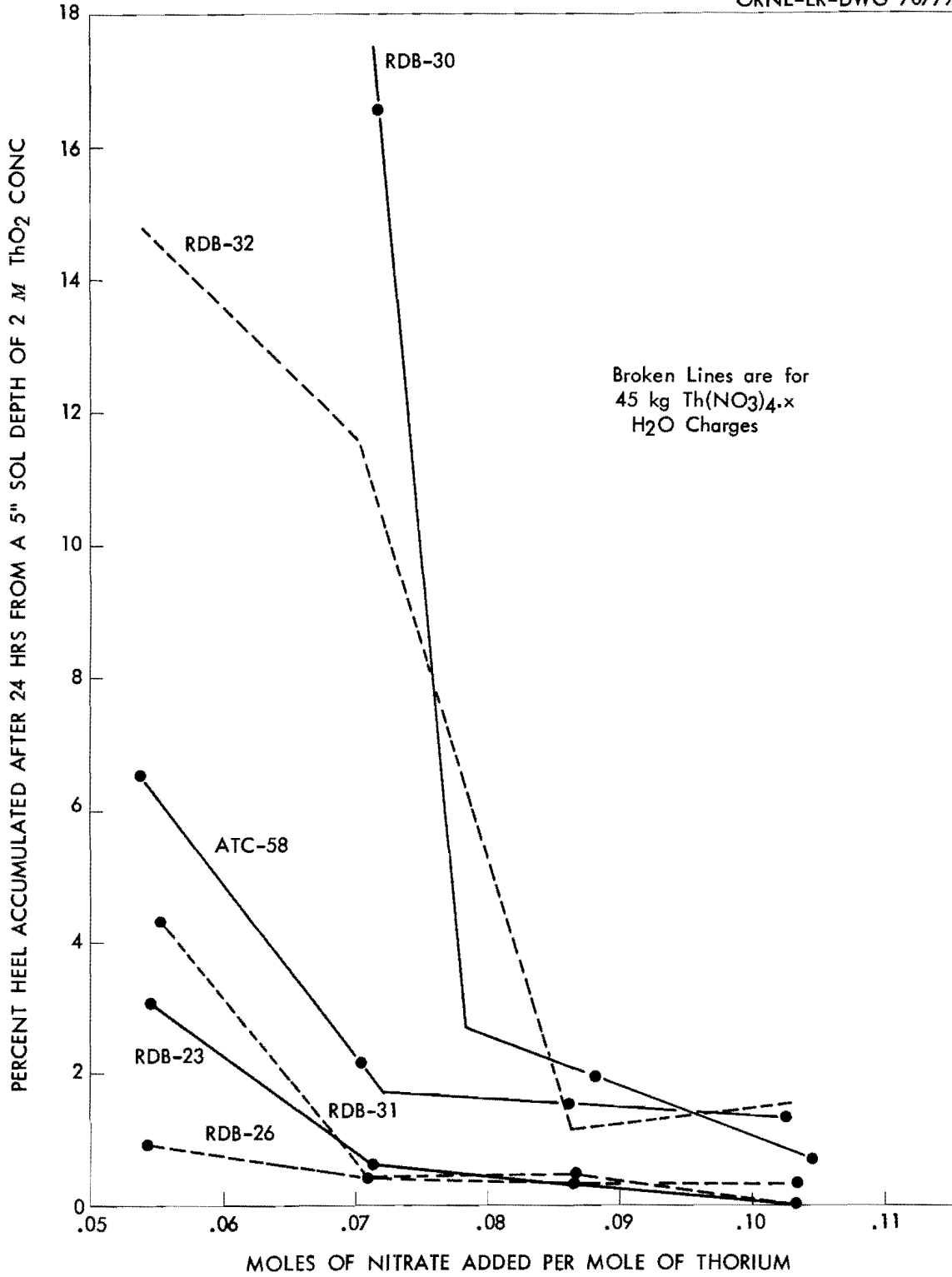Fig. 5.6. Rotating drum temperature vs. run time for Run RDB-30.

Fig. 5.7. Percent heel accumulated in 24 hrs for various steam denitrated products vs added nitrate to thorium mole ratio.

Rotary denitrator operating procedures are adequate to produce feed ThO_2 powders suitable for the BNL Kilorod program. One operator should be able to denitrate, disperse, decant and dispose of off-gas waste at a rate of 20 kg ThO_2 per day. At this throughput, one operator in a 5 day week should be able to produce sufficient thoria feed to supply the BNL Kilorod facility for one U-233 extraction charge or 10 days of plant operation.

5.3 Sol Preparation-Drying-Calcination Studies - C. C. Haws, D. A. McWhirter

Operation of the Kilorod scale equipment for sol preparation and oxide reduction was continued. Measures previously taken to seal the furnace were found adequate although gas usage is still high. Products having low O/U ratios (~2.02) and low gas releases (< 0.005 cc/g) were obtained. Two lots of material, prepared by addition of the wetted thoria slurry to a $UO_2(NO_3)_2$ solution, proved equal to materials prepared by the addition of ammonium diuranate to the thoria sols. The results of 6 runs made thus far in the Kilorod scale equipment are summarized in Table 5.4.

Beginning with Batch 4B, satisfactory O/U ratios and gas release values were obtained. Present Kilorod specifications require an O/U ratio of < 2.005 but this figure is not realistic and a revised specification of 2.02 ± 0.02 has been suggested. This has become necessary since analytically the lower limit of detection of this material corresponds to a ratio of 2.02, with an accuracy of this level of ± 0102. There is no present specification for gas release, but a value of < 0.01 g/cc is being considered.

The low values in Batch 4B were obtained by using gas flows through the furnace of ~120 cfh, while the results of runs 5 and 6 were obtained at lower gas flows (~30 cfh). Complete re-sealing of the furnace allowed the lower gas flow for the latter two runs. Argon and argon-hydrogen costs alone are about $3.00 per kg of product using present operating procedures (~35 cfh).

Samples from Batches 3B through 5A were reduced in a conventional hydrogen furnace using the 4% H_2-96% A mixture purchased for use in the Kilorod program. The O/U ratios and gas release values of these samples are equal to the last four values obtained in the Kilorod scale furnace. The latter furnace may therefore be assumed capable of maintaining the proper atmosphere at the 30 cfh flow rate.

Two methods of by-passing preparation of ammonium diuranate in the Kilorod cell have been suggested. The first of these methods was tested in run 6. The $UO_2(NO_3)_2$ solution was placed in the blend tank and the thoria powder (in a wetted state) was added directly. The nitrate content of the UNH was adequate for dispersion of the thoria. Ammonium hydroxide was then added to the sol to a pH of 3.1, or equivalent to neutralizing all nitrate in excess of an N/Th ratio of 0.12. The materials produced by this method are seen to be equal to the materials of the previous 5 runs which were made by ADU addition.

Table 5.4. <u>Properties of Sol-Gel Materials Produced</u>

<u>in Kilorod Scale Experiments</u>

Run No.	O/U Ratios		Gas Release Values (g/cc to 1200°C)		Vibratory Compaction Density[a] g/cc
	Kilorod Furnace	Lab H_2 Furnace	Kilorod Furnace	Lab H_2 Furnace	
1A	2.07		0.053		8.87
1B	2.12		0.049		
2A	2.06		0.034		8.83
2B	2.16		0.083		
3A	2.19		0.12		8.88
3B	2.18	2.03	0.11	0.001	
4A	2.22	2.05	0.068	0.002	8.97
4B	2.09	2.06	0.003	0.003	
5A	2.02	2.03	0.005	0.016	9.01
5B					9.03
6A	2.03		0.004		8.92
6B	2.03		0.003		8.91

[a]Vibrated in 1/2-in.-dia tube on 1-1/2-in. Branford vibrator.

Batches 5A and 5B were split into two equal portions, with one portion from each being crushed before firing. Both precrushed portions vibrated to 8.74 g/cc vs the 9.0 densities given in the above table for materials crushed after firing. The fines of the precrushed materials were not ball-milled, while the post-crushed materials were. The post-crushed portions yielded ~73% of the initial 6/16 fraction. This represents a maximum yield, however, which would be difficult to obtain in hot operations.

DISTRIBUTION

1.	L. G. Alexander (Y-12)	54.	A. P. Litman	
2.	E. L. Anderson (AEC Washington)	55.	J. T. Long	
3.	F. P. Baranowski (AEC Washington)	56.	B. Manowitz (BNL)	
4.	W. G. Belter (AEC Washington)	57.	J. L. Matherne	
5.	S. Bernstein (Paducah)	58.	J. A. McBride (ICPP)	
6.	R. E. Blanco	59.	J. P. McBride	
7.	J. O. Blomeke	60.	W. T. McDuffee	
8-11.	J. C. Bresee	61.	R. A. McGuire (ICPP)	
12.	R. E. Brooksbank	62.	R. P. Milford	
13.	K. B. Brown	63.	J. W. Morris (SRP)	
14.	F. R. Bruce	64.	J. W. Nehls (AEC ORO)	
15.	J. A. Buckham (ICPP)	65.	E. L. Nicholson	
16.	L. P. Bupp (HAPO)	66.	J. R. Parrott	
17.	W. D. Burch	67.	F. S. Patton, Jr. (Y-12)	
18.	W. H. Carr	68.	H. Pearlman (AI)	
19.	G. I. Cathers	69.	A. M. Platt (HAPO)	
20.	J. T. Christy (HOO)	70.	R. H. Rainey	
21.	W. E. Clark	71.	J. T. Roberts (IAEA, Vienna, Aust.)	
22.	K. E. Cowser	72.	K. L. Rohde (ICPP)	
23.	F. E. Croxton (Goodyear Atomic)	73.	C. A. Rohrmann (HAPO)	
24.	F. L. Culler, Jr.	74.	L. Rubin (RAI)	
25.	W. Davis, Jr.	75.	A. D. Ryon	
26.	O. C. Dean	76.	W. F. Schaffer, Jr.	
27.	D. E. Ferguson	77-79.	E. M. Shank	
28.	L. M. Ferris	80.	M. J. Skinner	
29.	R. J. Flanary	81.	C. M. Slansky (ICPP)	
30.	E. R. Gilliland (MIT)	82.	S. H. Smiley (ORGDP)	
31.	H. E. Goeller	83.	J. I. Stevens (ICPP)	
32.	M. J. Googin (Y-12)	84.	C. E. Stevenson (ANL, Idaho Falls)	
33.	H. B. Graham	85.	K. G. Steyer (General Atomics)	
34.	A. T. Gresky	86.	E. G. Struxness	
35.	P. A. Haas	87.	J. C. Suddath	
36.	M. J. Harmon (HAPO)	88.	J. A. Swartout	
37.	F. E. Harrington	89.	F. M. Tench (Y-12)	
38.	L. P. Hatch (BNL)	90.	V. R. Thayer (duPont, Wilmington)	
39.	O. F. Hill (HAPO)	91.	W. E. Unger	
40.	J. M. Holmes	92.	F. M. Warzel (ICPP)	
41.	R. W. Horton	93.	C. D. Watson	
42.	G. Jasny (Y-12)	94-123.	M. E. Whatley	
43.	H. F. Johnson	124.	G. C. Williams	
44.	W. H. Jordan	125.	R. H. Winget	
45.	S. H. Jury	126.	R. G. Wymer	
46.	K. K. Kennedy (IDO)	127-128.	Central Research Library	
47.	B. B. Klima	129-132.	Laboratory Records	
48.	E. Lamb	133.	Laboratory Records (RC)	
49.	D. M. Lang	134.	Document Reference Section	
50.	S. Lawroski (ANL)	135.	Research and Development Division	
51.	R. E. Leuze	136.	ORNL Patent Office	
52.	J. A. Lieberman (AEC Washington)	137-		
53.	R. B. Lindauer	151.	DTIE	